Characterization of Fresh and Hardened Properties of 3D Printable Cementitious Materials Produced with Ground-Granulated Blast-Furnace Slag

by

Mohamad Basel Shoueb

A thesis
Presented to the University of Waterloo
in fulfillment of the
Thesis requirement for the degree of
Master of Applied Science
in
Civil Engineering

Waterloo, Ontario, Canada/ 2021

Examining Committee Membership

Professor. Hassan Baaj (Supervisor)

Professor. Maria Anna Polak (Supervisor)

Professor. Adil Al-Mayah (Second Reader)

Professor. Shunde Yin (Third Reader)

Author's Declaration

This thesis consists of material all of which I authored or co-authored: see Statement of Contributions included in the thesis. This is a true copy of the thesis, including any required final revisions, as accepted by my examiners. I understand that my thesis may be made electronically available to the public.

Abstract

Application of additive manufacturing technology to promote the digital construction practice in civil engineering has been gaining momentum, especially during the past 5 years. To this end, three dimensional concrete printing (3DCP) for structural elements has been the focus of several research groups around the globe. A comprehensive review of the existing literature was conducted as the first stage of this study with a focus on the fresh concrete properties, and deposition platform.

Review of the literature indicates that in almost all of the published research, fly ash has been dominantly used as the supplementary cementitious material (SCM) in additive manufacturing of concrete mixes. However, fly ash is not domestically available in the majority of Canadian provinces, except for specific west coast areas, and hence is typically an imported material from the U.S. Since the fly ash is not a domestic material, its use leads to significant increase in the cost of 3D-Printed concrete mixes in Canada. On the other hand, proper use of concrete admixtures is a key when designing a printable concrete mix. Among the several admixtures that can be used such as accelerators, retarders, water reducers, and air-entraining agents; high range water reducers (a.k.a. superplasticizers) are considered essential. The existing literatures in this area of technology have not addressed the effect of powder formed high range water reducers on the hardened properties for both cast and printed concrete or on the printability. Furthermore, the literature review reports contradictory findings in terms of the compressive and flexural strengths of cast specimens as compared to those of the printed specimens. In addition to these contradictory reports, the specimen dimensions used for such testing were not large enough to represent the effect of bond strength between the printed layers on the hardened concrete properties. It should also be noted that the stress-strain curves are not provided in almost all the materials published at the time of writing this paper. The lack of such information is considered a hindrance for successful modeling of 3D printed concrete objects using numerical methods such as finite element method (FEM). Developing a high performance 3D printable concrete mixes through the use of the domestically raw materials in Ontario and Canada was set as the primary goal, therefore, Ground Granulated Blast Furnace Slag (GGBFS) had been chosen as a cement replacement along with the use of powder superplasticizers. The experimental results had shown the mixes with GGBFS up to 39% along with a specific range of superplasticizer dosages have

resulted in high-performance 3D printable mixes. However, the printed specimens exhibited sever anisotropic material behavior and reductions in compressive and flexural strengths comparing with the cast specimens.

In robotic side, the developed platform at the University of Waterloo includes a six-degree of freedom robotic arm, a combined mixer and pump system, a replaceable nozzle connection, and safety cages. The system could be programmed to execute complicated shapes and printing patterns and is synchronized with a duo system to maintain a steady supply of materials proportional to the printing pace and interruptions. The selected system has the capability of being used in both laboratory and actual job site environments. To minimize the materials usage, the system was selected to run on dry ingredients (including sand, cementitious materials, and powder-form admixtures) with the water being added separately. Therefore, the production could be stopped at any point without the need to discard a considerable amount of mixed materials as it commonly happens in conventional construction practices.

Acknowledgments

I wish to express my sincere thanks to my supervisors Prof. Hassan Baaj, and Prof. Maria Anna Polak for their supports, guidance, and encouragement during my master study. I would also like to express my sincere appreciation to the committee members of my defense Prof. Adil Al-Mayah and Prof. Shande Yin from the University of Waterloo.

I would like to acknowledge CEE Department's staffs: Victor Lewis, Peter Volcic, Richard Morrison, and Douglas Hirst for their efforts and safety support and guidance.

My gratitude goes to all my colleagues at the University of Waterloo for the wonderful and enjoyable moments we shared.

I dedicate my efforts to my beloved family in Syria. I am so grateful and honored to be son of such great parents (Dad: Bassam Shoueb, Mom: Wafaa Saada). In addition, I am so grateful to be surrounded with great and supportive siblings (Brother: Alaa Al- deen Shoueb, Sister: Alaa Shoueb). You being with my side has helped me to reach where I am today.

Thank you all

Table of Contents

Table of Contents

List of Figures

List of Tables

Chapter 1: Introduction

Additive manufacturing (AM), also known as three-dimensional printing (3DP), has the advantages of higher building efficiency, lower labor cost, and less construction wastes as compared to the traditional construction technology. 3D-printed concrete is a special type of concrete, deposited layer by layer through the use of 3D printer and without any formwork support and vibration process. The most important performance indicators for 3DPC, such as workability, setting and hardening time, and mechanical properties, can be optimized by adjusting printing parameters and raw materials selection.

To date, a few building structures have been successfully printed using the 3D printed concrete technology either for demonstration purposes or for real-life use. The 3D printed concrete has a great potential on practical applications, such as the affordable housing construction in low-income countries, military bunkers, and complex constructions where the formwork is difficult to manufacture.

1.1 Background

In the 1980's, the first additive manufacturing systems were envisioned using novel liquid photopolymers which could be cured using focused stereo lithography lasers in a vat (ELLIOTT & WATERS, 2019). By the mid-1990's, these systems gained popularity for industrial applications and the 3D printing of lithographic polymers came to the forefront of an entirely new industry. Nowadays, modern polymer 3D printing industry is dominated by the "fused deposition method" or "material extrusion" technique due to the ability of thermoplastic polymers to be melted and extruded at relatively low temperatures (ELLIOTT & WATERS, 2019).

Additive manufacturing has become valuable in the bio manufacturing, medical device, and aerospace industries to produce one-off custom solutions for unique problems without creating unnecessary waste (Paul, Tay, Panda, & Tan, 2018). Research into the additive manufacturing techniques as well as the use of non-liquid materials has allowed for the creation of a variety of 3D printing processes (ELLIOTT & WATERS, 2019). Table 1-1 summarizes the available Additive Manufacturing (AM) techniques for all classes of materials.

Table 1-1. Additive manufacturing techniques for polymers, metals and ceramics (ELLIOTT &

WATERS, 2019).

Material Class	Available Techniques
Polymers	• Stereo lithography Printing using Vat polymerization (VP) • Fused Deposition Modeling (FDM)/ Material Extrusion • Laminated Object Manufacturing • Powder Bed Fusion using Selective Laser Melting (LM) or Electron Beam melting (EBM) • Material Jetting
Metals	• Selective Laser Sintering (SLS) • Binder Jetting • Material Jetting • Directed Energy Deposition (DED) • Large-scale Material Extrusion (e.g. Big Area Additive Manufacturing, Tennessee, USA)
Ceramics	• Binder Jetting • Material Jetting

Furthermore, the use of multi-axis Computer Numerically Controlled (CNC) devices have allowed industrial designers to autonomously produce increasingly complex geometries which could not be possible through conventional manufacturing techniques; this ability was especially significant in the field of rapid prototyping as AM techniques do not require costly molds. Consequently, the popularity of this technique has decreased the cost-of-entry for the polymer extrusion technologies to a point where hobbyists can use at-home 3D printers to create both functional and decorative prints with relative ease (ELLIOTT & WATERS, 2019).

From construction perspective, concrete is considered the most durable material among others to be used for construction purposes. However, the concrete that has been used in AM applications is considered to be a special material as it requires to meet certain strict requirements at fresh, early-age, and hardened state, which makes its design a challenging task. Since the traditional technology, including setting up formworks and vibrating are not required for 3D-Printing, the 3D printed concrete combines the advantages of extruding and self-compacting concrete without any needs for molds as it is designed to stand by itself (Zhang, Jialiang, Dong, Xun, & Han, 2019). Figure 1-1 and Figure 1-2 show layer fabricated technology that uses robotic arms and extrusion nozzles using a concrete material as an ink for 3D- Printer to build walls (Ghaffar, Fan, & Corker, 2018)

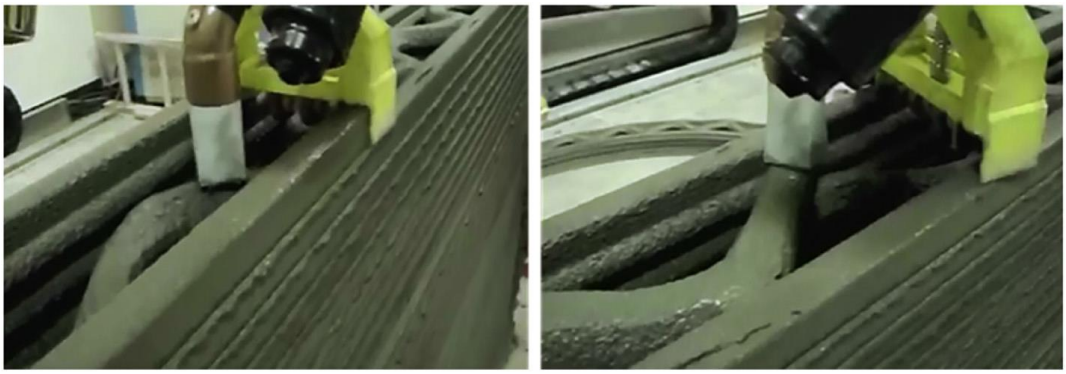

Figure1-1, 3D-Printed concrete with cross patterns (Ghaffar, Fan, & Corker, 2018)

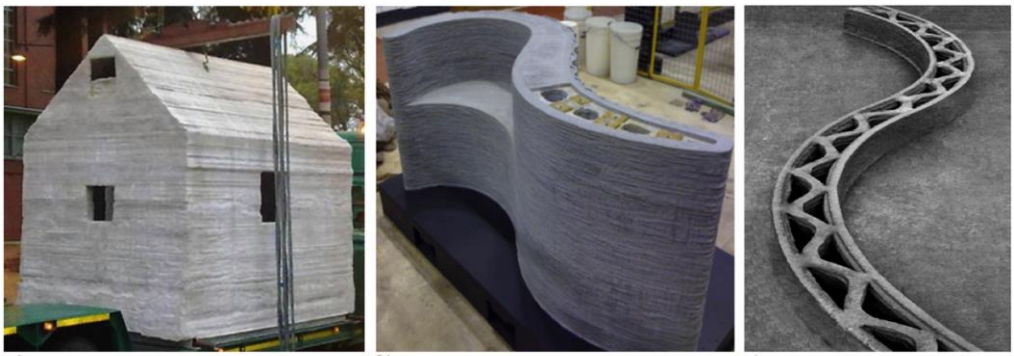

Figure1- 2, 3D-Printed objects a) large scale object, b) curved wall, and c) Contour Crafting curved wall (Ghaffar, Fan, & Corker, 2018)

1.2 Problem Statement and Objectives

Design of a 3D printable concrete material remains as a challenging task. Currently, there are no specific guidelines or specifications that lay out the necessary steps required for a printable concrete mix. The main roots of this challenging nature can be named as: 1) the lack of historic data or an extensive documented experience with this innovative material in civil construction; 2) specific nature of the material which requires optimization of its properties to simultaneously meet strict requirements at fresh, early age, and hardened states; 3) concerns about the quality of bonding between consecutive layers and the directional properties of the hardened concrete; and 4) high dependency of the properties on the extrusion mechanism, equipment, printing job layout, and source of raw materials.

To this end, developing an acceptable 3D printable concrete through the use of the domestically raw materials in Ontario and Canada was set as the primary goal in this research.

Review of the literature indicates that in almost all the published research, fly ash has been dominantly used as the Supplementary Cementitious Material (SCM) in additive manufacturing of concrete mixes. However, fly ash is not domestically available in the majority of Canadian provinces, except for specific west coast areas, and hence is typically an imported material from the U.S. Therefore, since the fly ash is not a domestic material, its use leads to significant increase in the cost of 3D-Printed concrete mixes in Canada.

On the other hand, proper use of concrete admixtures is a key when designing a printable concrete mix. Among the several admixtures that can be used such as accelerators, retarders, water reducers, and air-entraining agents, high range water reducers (a.k.a. superplasticizers) are considered essential. To this end, it is crucial to understand the effect of a specific superplasticizer on both fresh and hardened properties of concrete mixes. Furthermore, the physical form of the superplasticizer, either liquid or powder form, may have to be determined depending on the type of equipment used in the printing process. Use of powder superplasticizers can offer great advantages for this purpose, and was hence studied in this research. The existing literature in this area of technology has not addressed the effect of powder formed high range water reducers on the hardened properties for both cast and printed concrete or on the printability.

Finally, the literature review reports contradictory findings in terms of the compressive and flexural strengths of cast specimens as compared to those of the printed specimens. In addition to these contradictory reports, the specimen dimensions used for such testing were not large enough to represent the effect of bond strength between the printed layers on the hardened concrete properties. It should also be noted that the stress-strain curves are not provided in almost all the materials published at the time of writing this thesis. The lack of such information is considered a hindrance for successful modeling of 3D printed concrete objects using numerical methods such as finite element method (FEM).

The global objective of this study is to provide an insightful review on the effect of superplasticizer on the printing quality and the hardened concrete properties of cast and printed concrete properties at different ages (1, 7, 28) days. The outcomes of the study are:

I. The effect of using Slag as supplementary cementitious materials along with different dosages of superplasticizer and water cement ratios on the printing quality and the hardened concrete characterizations.

II. Identifying the desirable rheological values of fresh concrete by using shear strength as an indicator to come up with printable mixes.

III. Optimizing the superplasticizer's ratio in concrete mixes to produce with high performance hardened concrete properties.

IV. Providing a comprehensive comparison between the cast specimens and the printed ones in terms of compressive, flexural and bond strength by scaling the size of printed samples to simulate the cast ones.

V. Developing 3D- printing platform at the University of Waterloo.

1.3 Research Motivations

Despite the wealth of experience with traditional building methods, there are several disadvantages including slow construction speeds and variability in construction quality, especially when it comes to using concrete as a construction material. One issue is that the concrete needs time to harden and strengthen which can lead to a sharp increase in the cost of building, and methods to accelerate that process can lead to potential shrinkage cracking if the concrete mix is not properly designed. Traditional concrete construction also requires molds to cast the concrete which can account for up to 40 to 50% of the total cost of construction. In addition, the construction process is more involved and may require hiring higher-skilled designers and builders which can further add to construction costs. On the other hand, 3D printing of structures using printable concrete mixes can offer advantages over the traditional construction practices. The main advantages of using AM for construction purposes are as follow:

1. Consistent quality as less workers are required which minimize the human errors.
2. Significant increase in the speed of construction [Up to 150 to 200 mm/s]
3. Environment friendliness as no molds are required which mean less wasted materials
4. The ability to work under different conditions, especially in severe weathers like Canadian weather.

Combine all the mentioned factors could lead to drop the cost of construction by 40 to 70%, and that could reflect on affordable houses and friendly environment constructions.

Chapter 2: Literature Review

2.1 Types of Additive Manufacturing

A brief overview of the different types of additive manufacturing processes is provided here, focusing on the state of the material before deposition and according to its relevance to the additive construction process. Figure 2-1, shows the different states of a material before deposition (Labonnote, Rønnquist, Manum, & Rüther, 2016). The potential relevance and possible applications of each additive manufacturing process in relation to additive construction are briefly discussed.

- Additive manufacturing processes based on solid-like materials:

  These involve the layer-wise assembly of material in a solid form. Bonding between the different layers is achieved by a number of different methods, such as by the use of a glue-like material, or as an integral part of the assembly process itself e.g., weaving. Masonry is probably one of the oldest additive construction processes based on solid-like materials. Building a brick wall using mortar to bond the layers was an additive manufacturing process well before the development of 3D printers. Other innovative processes such as the 3D-weaving of carbon fibers have been used in applications from vehicle body frames to critical aircraft parts (Shelley, 2006), and can be envisaged as a means of producing highly optimized building components.

- Additive manufacturing processes based on viscous- like material:

  This involves the deposition of material in a viscous liquid form. They are, thus, also referred to as “Extrusion-based processes”. Solidification of the material is achieved by curing following extrusion. AM based on viscous material is the most investigated additive construction process. Relevant materials commonly comprise a combination of paste and bulk materials. Bulk materials may be composed of:

  - Natural aggregates such as soil, sand, natural gravel, crushed stone, clay or mud.
  - Recycled aggregates such as those from construction, demolition or excavation waste.
  - Manufactured aggregates such as air-cooled blast furnace slag and bottom ash.

- Natural fibers, such as cellulose and recycled wood fibers.

Bulk material is combined with a binding paste that may be composed of:

- Cements consisting of mixtures of oxides of calcium, silicon and aluminum.
- Polymer blend (Labonnote, Rønnquist, Manum, & Rüther, 2016).

Both contour crafting (Khoshnevis, 2004) and freeform construction have been using this process extensively for concrete type materials (Buswell, C. Soar, AGibb, & Thorpeb, 2007).

- Additive manufacturing processes based on powder-like materials:

This involves transforming a material from a powder to a solid state, which can be achieved by either melting or sintering, enabled by an energy source, or curing by means of a chemical reaction. The powder- feed process has been applied in additive construction by developing a powdered concrete mix, subsequently cured by hydration using an ink jet spray (Rael & San Fratello, 2011). Sintering, melting and exothermic chemical reaction have also been investigated for additive construction application in extra-terrestrial environments (Wilhelm & Curbach, 2014), (Krishna , Roberson , O'Connor, Trigwell, & Bose, 2012)

- Additive manufacture based on liquid- like materials:

This involves transforming a material from a liquid to a solid state. Curing is achieved by means of a light source. So far, no application of this form has been investigated for civil engineering construction purposes.

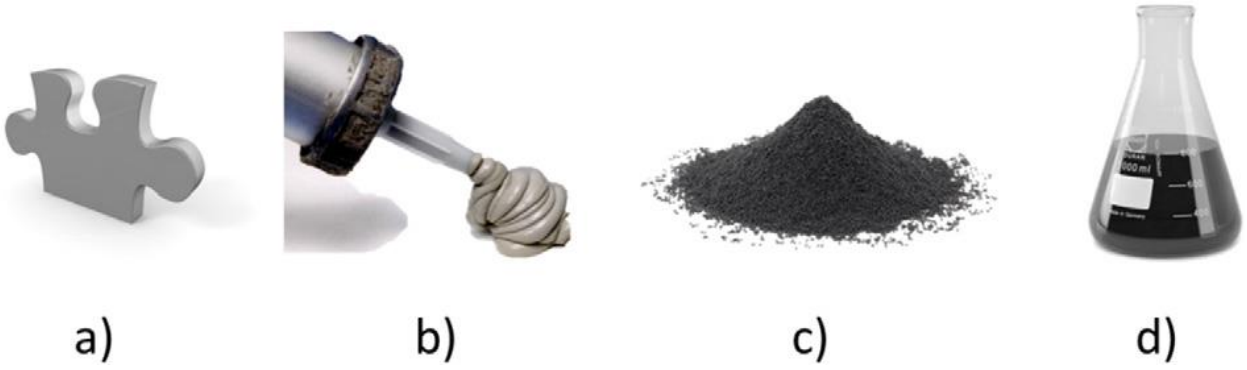

Figure 2-1, The different states of materials before deposition, a) solid like, b) viscous like c) Powder like, d) Liquid like (Labonnote, Rønnquist, Manum, & Rüther, 2016)

Materials that are used in additive manufacturing are required to meet sometimes contradictory requirements related to desirable properties for an efficient additive manufacturing process and the construction conditions.

2.2 3D-printing for Building Construction Purpose

AM technology can have the potential to help construction industry to transition into a responsive and advanced sector, although, different grades of advanced printable feed-stocks need to be formulated/developed to make this technology more effective for the making of structural elements. The generalized perception is that AM is most relevant for industries where the demand in customization, flexibility, design complexity, and the cut on high transportation costs for the delivery of end products is crucial, therefore, making the construction industry a potentially lead beneficiary of the next Industry 4.0 revolution. The simple approach of layer-wise construction is a process that has already been practiced for a long time in the building sector, such as the conventional brick layering techniques. The true novelty for advanced construction technology is to combine new highly efficient and sustainable materials along with the most advanced tools of the digital age, using architectural design software as the front end and combine different components of robotic technology to automate and excel processes that have been proven manually. Thorough testing is essential to improve the way construction industry works by using cutting-edge technology to enhance the ability to anticipate and adapt (Ghaffar, Fan, & Corker, 2018).

In 1997, the first attempt of using additive manufacturing approach for construction purposes suggested by Penga. He replaced a massive complexity of information processing that are required in construction with a large number of simple elemental operations which can be easily controlled by computer to produce small masonry structures using a selective deposition of alternating thin layers of sand and Portland cement that were cured with steam (Penga, 1997). Figure 2-2, demonstrates the masonry layout and the printed sample.

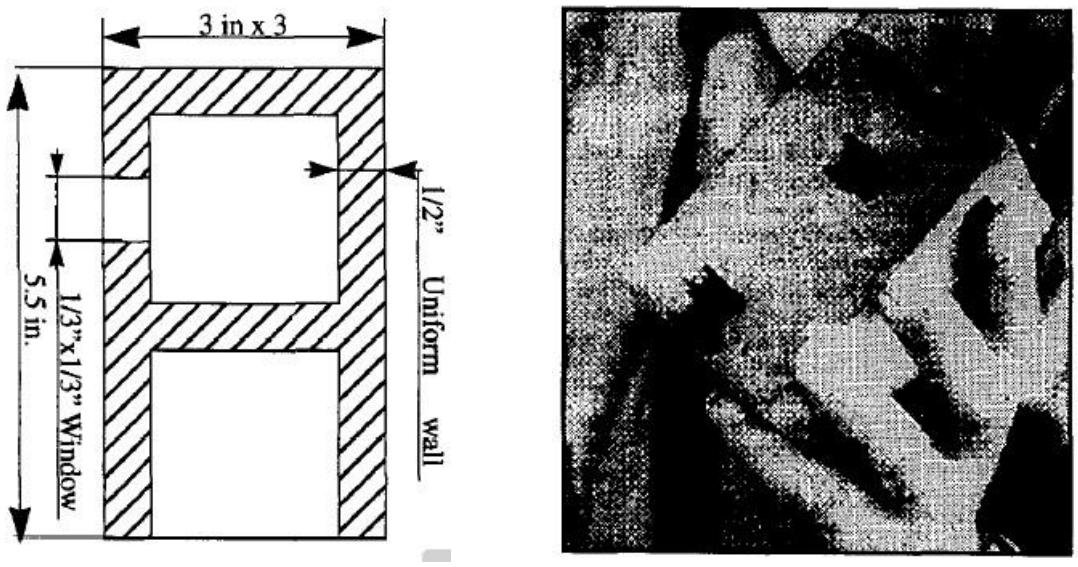

(a) (b)

Figure2-2, a- Masonry layout, b- 3D Printed masonry (Penga, 1997)

According to literatures, the two main parameters controlling the process of the 3D printing are the printing machine, and the printing ink, which accordingly could determine the kind of product produced by the process (Tofail, et al., 2017). Currently, for construction purposes, there are three main categories that all the trials will fall under: contour crafting method, D-Shape method, and concrete printing method (T, et al., 2012). Each of the above processes will have a different objective, and then different forms of application.

2.2.1 Contour Crafting (CC)

Contour crafting was founded at the University of Southern California by Behrokh Khoshnevis in 2005. In this type of construction process, a specific amount of mortar mixture is delivered to make the desired objects. Mortar mixture is added in a layer by layer manner with a certain time delay between successive layers (Hwang & Khoshnevis, 2005). Contour crafting is also known as an additive technology that uses computer control to exploit the superior surface-forming capability of troweling to create smooth and accurate planar and free form surfaces. Some of the important advantages of CC compared with other layered fabrication process are: 1) better surface quality, 2) higher fabrication speed and 3) a wider selection of materials (Khoshnevis, 2004). Figure 2-3, demonstrates the contour crafting technology for construction purposes.

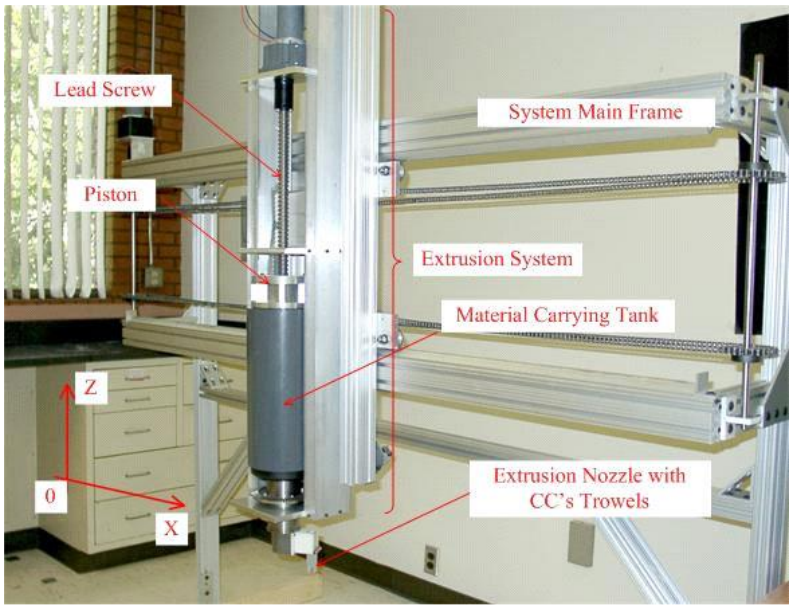

Figure2-3, Developed Contour Crafting for construction purposes (Khoshnevis, 2004).

Once the system completes one-layer cycle, the entire extrusion assembly moves vertically an incremental distance equal to the height of the layer's thickness. The cycle is repeated until the final shape of the boundary is established. The machine frame has two rails with V Shape profiles that guide the extrusion system. Figure 2-4, a 3D-printed concrete wall with a desired span and height that was produced by contour crafting machine. Figure 2-5, demonstrates different types of 3D-Printed object that could be achieved using Contour Crafting machine (Khoshnevis, 2004).

Since 2002, several projects have been published to design 3D dome-shaped buildings with massive construction. Pioneers are space agencies NASA and ESA, who intend to use automated 3D printing technology for construction of the bases as the first step of the exploration of Moon and Mars. As a part of NASA research, the scaled 3D printed dome was printed by CC using horizontal slicing.

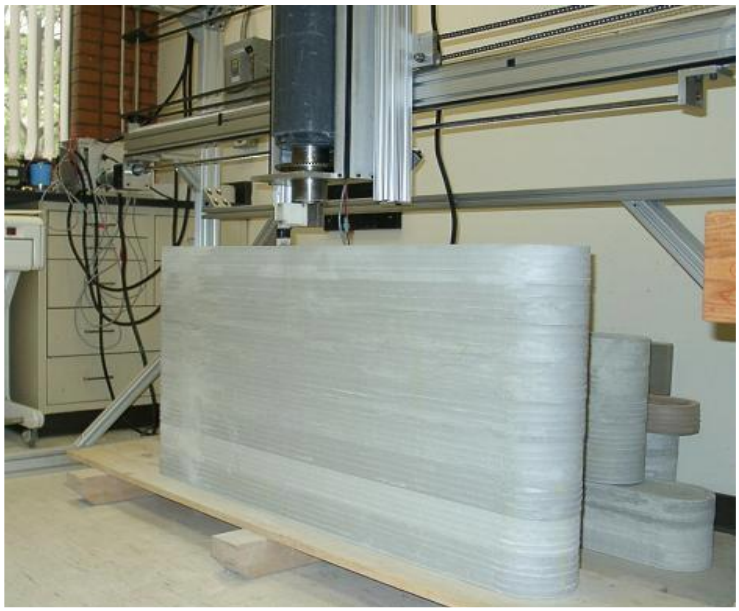

Figure2-4, 3D- printed concrete wall fabricated by CC machine (Khoshnevis, 2004)

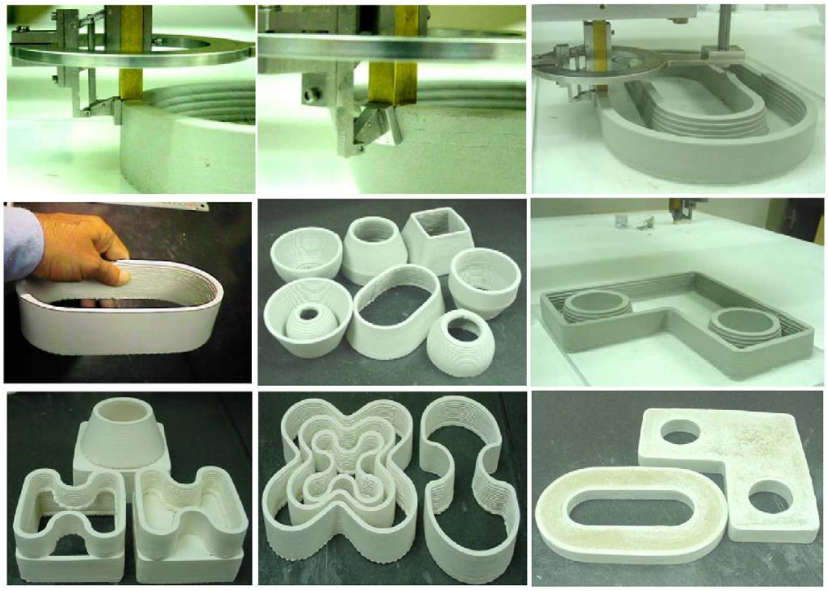

Figure2-5: Different 3D- printed objects fabricated using CC machine (Khoshnevis, 2004)

When using horizontal layers, in the cap part layers cannot deal with the staircase effect, so it is not clear from the available pictures, how the top part of the model was fabricated (KOVÁŘÍK, SVOBODA, & ACHTEN, 2019). Figure2-6, demonstrate a prototype of lunar project built with CC technology by Contour Crafting Corporation.

Figure2-6, Lunar project built with CC Technology (KOVÁŘÍK, SVOBODA, & ACHTEN, 2019)

The contour crafting method is targeting the printing speed and productivity, so it is a low-resolution printer that is the most common method and what experts are aiming to develop further for mass production and mass construction. Due to high speed of printing, a certain limitation over material strength and building shapes are associated with this method (Jianchao, Zhang, Faried, & Wengang, 2017).

2.2.2 D-Shape Technology

The D-Shape technology was invented by Enrico Dini in 2006. D-Shape is a method of -digital construction that uses a binder jetting 3D printer for architecture. Figure 2-7, demonstrates D-shape technology for construction purposes. This technology materializes buildings directly form computer via a process of alternating layers of granular material and writing on them with an appropriate ink binder that turns the granular material into shapes. It deposits any mix granular material and fibers in a range of diameter starting from 0.1 to 4 mm and any ink binder having a viscosity between water and a slurry. The nozzles of the D-shape printer head deposits drops of ink binder whose volume are about 100 times bigger than existing inject printer heads. Seen form the outside, the D-Shape appears as a portal structure which supports a peripheral frame raised along four columns. On the frame there are two gantries, one of them distributes and spreads a granular material, while the second holds a multi-binder jetting print head. D-Shape is designed to be multi material and multi binder. The granular material might be form almost any king of nature, while the binder may be an aqueous solution of different additives. The gantry distributer is

powered by a feeding system of granular material from the ground, while the print head is fed by a tank and by a hydraulic system. Regarding the D-Shape operation, a personal computer supervises all control operations of the machine. The Process can be automatic, but the presence of at least one operator and a few assistants is mandatory (Dini, 2006). One of the most interesting projects done by Enrico using D-Shape technology is "The Radiolaria Pavilion" which is an organic open cell designed by Andrea Morgante, Figure2-8, depicts Radiolaria Pavilion.

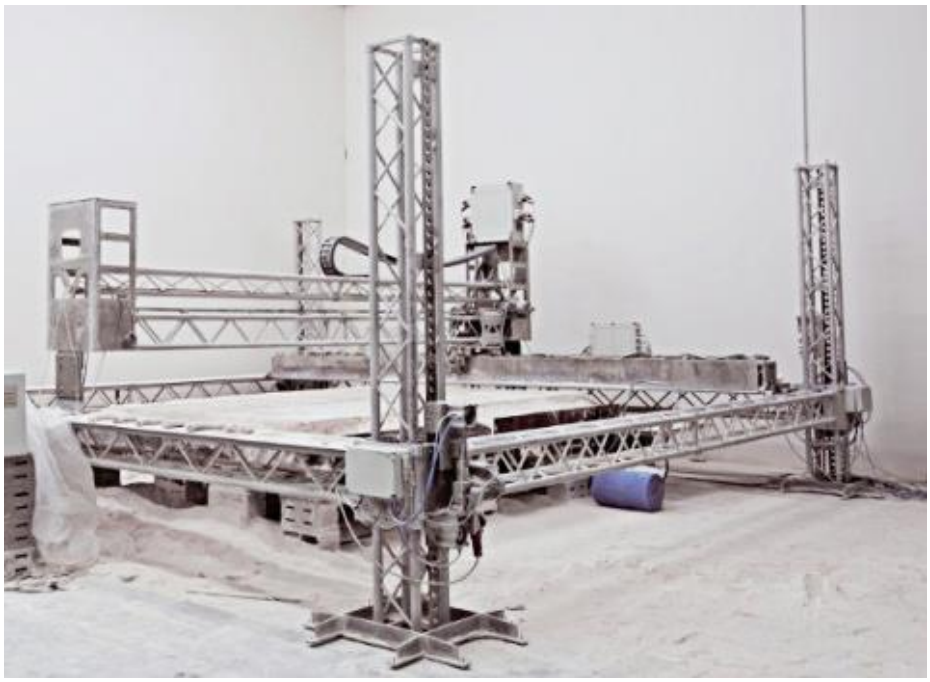

Figure2-7, D-Shape machine for construction purposes (Dini, 2006)

This method is very slow, but it can produce both high resolution and complicated objects, especially as it uses the loose material as a bed to support the suspended and horizontal surfaces (Jianchao, Zhang, Faried, & Wengang, 2017).

Figure2-8, Radiolaria pavilion fabricated by D-Shape technology (Dini, 2006)

2.2.3 Concrete Printing

The third category of 3D-printing machines are called concrete printers. Concrete printers using the same method of Contour Crafting one, where the materials are pre- mixed before the printing begins (Jianchao, Zhang, Faried, & Wengang, 2017). The process starts with data preparation which is similar to the most of the additive manufacturing processes. The geometries are sliced into horizontal layers with fixed cross section dimensions that comply with nozzles size. The data of the sliced layers generated from a 3D CAD model are saved as G-code format. These instructions are read by the machine that operates all the control commands adjusting the nozzle position, movement and material flow, etc. The prototype machine illustrated in Figure 2-9 consists of a 5.4m (L) by 4.4m (W) by 5.4m (H) frame and a printing head on a mobile horizontal beam which moves in Y and Z directions, while the printing head moves in the X direction.

Figure2-9, Concrete printing technology (Jianchao, Zhang, Faried, & Wengang, 2017)

The printing process after the data preparation consists of three steps: materials preparation, delivering, and printing (Lim, et al., 2009). The main differences between Contour Crafting and Concrete printing could be summarized in three points: Concrete printing has a lower resolution and a lower speed, which allows the concrete to have a higher strength. However, the low printing speed is considered a major limitation regarding the productivity and object size (Jianchao, Zhang, Faried, & Wengang, 2017). Figure 2-10demonstrate 3D- printed object done by concrete printing, the left Figure (2-10, a) shows a lower resolution due to the big size of the nozzle (i.e., 22mm by 15 mm), while by going with smaller nozzle sizes (e.g., 9 mm by 6 mm) as can be seen from Figure (2-10, b) the resolution was better.

a 

b 

Figure2-10, Printed objects by concrete printing technology (Jianchao, Zhang, Faried, & Wengang, 2017)

2.3 Type of Errors in Layered Manufacturing

For additive manufacturing to be accepted as one of the main methods in construction field, parts that are created by AM have to consistently satisfy the critical geometric tolerances and should be accurate. Accuracy in additive manufacturing is evaluated by dimensional errors, form errors and surface roughness of manufactured parts. Layered manufacturing (LM) is considered as a member of the AM family. LM has been quickly adopted by industry in the past decade due to the low volume prototype production. However, LM process has its own drawbacks that limit their applicability. Form errors is common error that is faced in AM. The creation of form errors in parts manufactured by LM depends on the specifications that are chosen by the designers. Form errors could be included in three types of errors flatness and straightness errors, cylindricity errors, and Staircase errors. The staircase error has been the major concerns for construction industry to be widely adopted as one of the main construction technologies. It will not only worsen the surface quality but also create errors on the built parts. LM approximates the objects by layers with vertical edges; the stacking of the layers does not match the original cad model very well, thus causing what is called staircase error. Figure 2-11, demonstrates the staircase error in the layered manufactured surfaces (Singh, 2014).

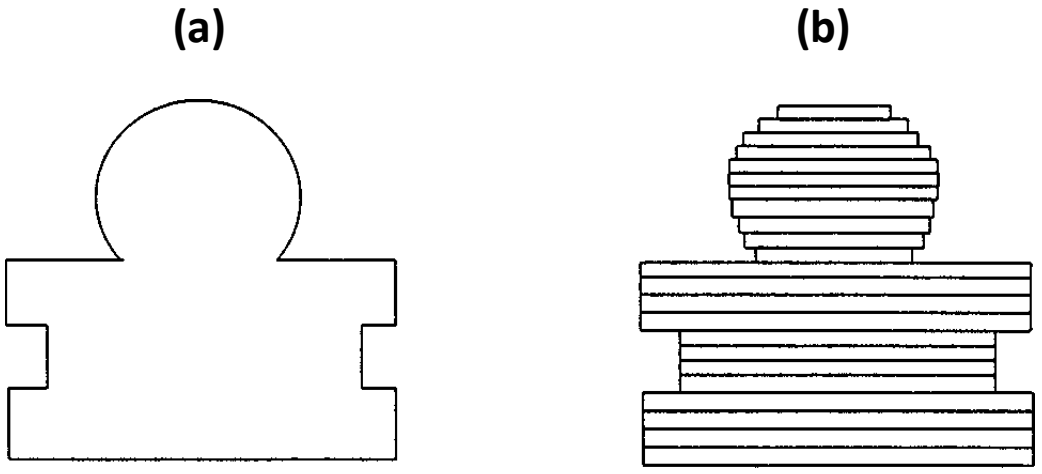

Figure 2-11, a- Cad model, b- Layered manufactured model with staircase effect (Singh, 2014).

The extent of staircase effect depend on the layer thickness and the relative orientation of the build direction and the geometry of the curved parts in the layered manufactured object. The staircase effect error is closely related to the layer thickness. The staircase error increases with the

layer thickness, and by using an adaptive slice method the staircase error could be minimized. An adaptive slicing algorithm is a method where the layers thicknesses are varied in order to match as much as possible the geometry CAD model or the actual one. Figure 2-12, demonstrates layered dome using adaptive approach slicing versus slicing with equal layer thickness (Singh, 2014).

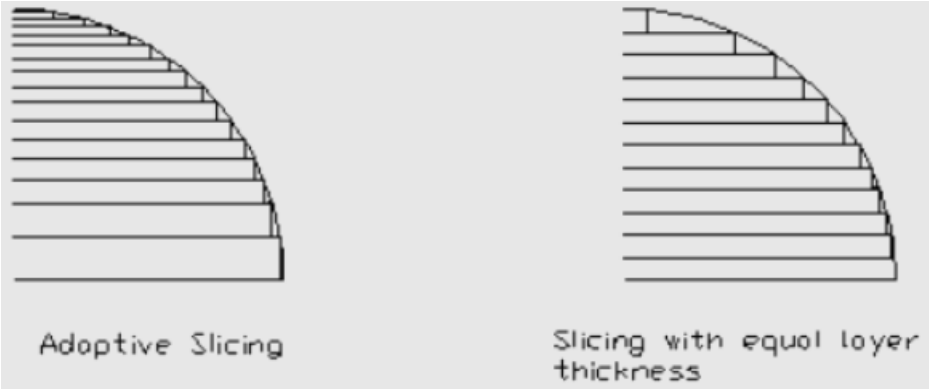

Figure2-12, Adaptive slicing vs equal layer slicing (Singh, 2014)

Other approach to minimize the staircase effect is to reduce the layer's thickness but that reflect in a longer time to build the object. Figure 2-13, shows a layered dome with different thicknesses. It can be noticed the formation accuracy of layered dome is increased with lowering down the layer height. Figure 2-14, shows how the effect of using thinner layer on build time. The figure implies that there is a trade-off between the accuracy of the produced object and the building efficiency. The accuracy and minimizing the errors can be especially important in case of dome shaped structures and curved patterns. Such trade-off needs to be carefully considered when planning the printing layout of either a full structure or a single element (Singh, 2014).

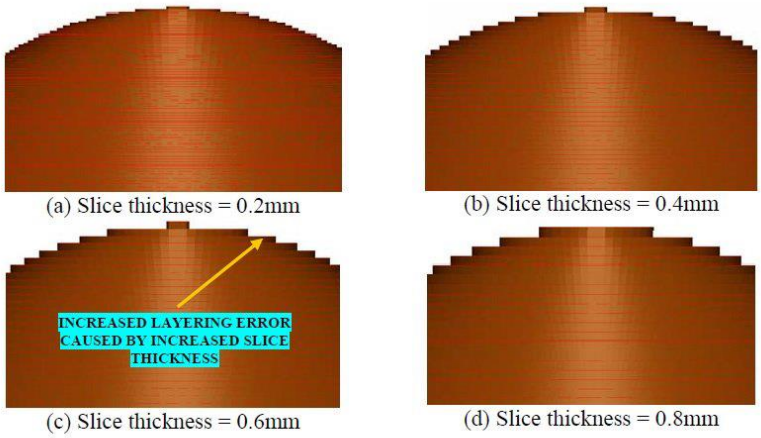

. Screenshots of Sliced Sphere STL Files

Figure2-13, The effect of slice thickness on the layering error (Singh, 2014)

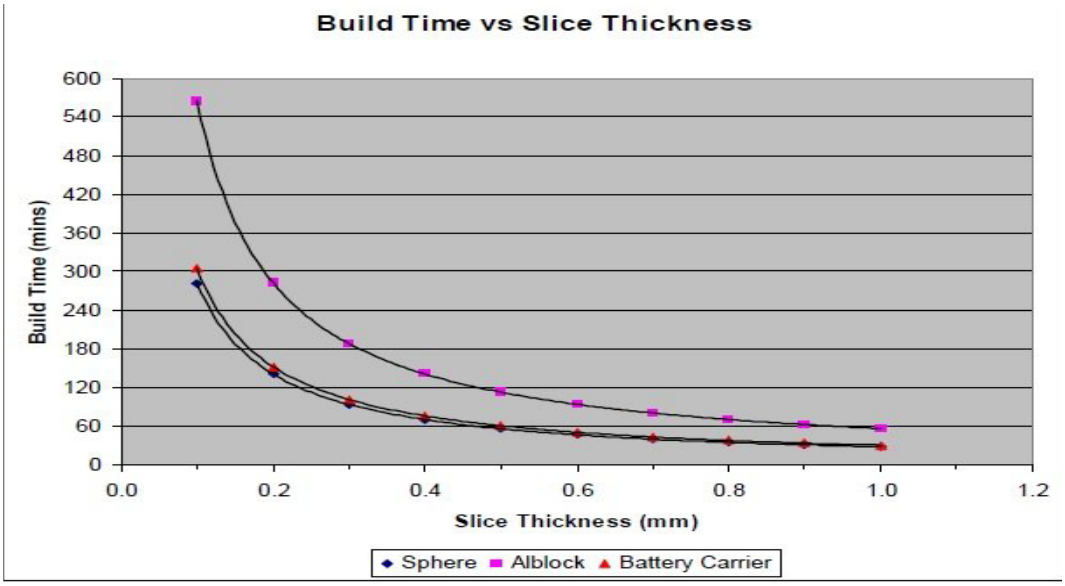

Figure2-14, Build time versus Slice thickness (Singh, 2014)

2.4 3D-Printed Projects Worldwide

Across the industry, there are some impressive projects worldwide considered a revolution in additive manufacture in construction field. Some of the additive manufactured projects that are recently done are listed here.

In 2015, DUS Architects designed and built a 3D-printed “Urban Cabin” which is a mini-retreat in the midst of Amsterdam. This Cabin is one part of a research project focusing on compact and sustainable housing solution in urban environments and aimed to display how 3D printing can offer solutions for disaster relief and temporary functional housing. The total volume of tiny 3D printed house is up to 25 cubic meters of sustainable bio-plastic materials within 8 square meters, includes a porch and a sofa that transforms into a twin bed. The project was fabricated using FDM 3D printing. Figure 2-15, demonstrates the 3D- printed urban cabin for disaster refugees (Carolo, 2020).

In 2015, Lewis Yakich the owner of Lewis Grand hotel in Philippines with a help from Andey Rudenko, built a 3D- printed hotel extension, including bedrooms, living rooms and a Jacuzzi room. The 130 square meter extension took over 100 hours to be printed. Building materials were a combination of sand with volcanic ash, resulting in stronger walls and improved bonding strength between layers. He claimed that the 3D-printed project saved him 60% of the building cost (Carolo, 2020). Figure2-16, shows a 3D-printed hotel extension by Lewis Yackin

Figure2-15, 3D-Printed Urban Cabin in Amsterdam (Carolo, 2020).

Figure2-16, 3D-Printed hotel's extension by Lewis Yakich (Carolo, 2020).

In 2016, an architectural firm called Gensler designed and built "Office of the future" for the United Arab Emirates National Committee as the headquarters for the Dubai Futures Foundation. The total area of 3D printed objects reach 2600 square foot. The office is composed of concrete components printed with a 20 foot high, 120 foot long, and 40 foot wide. Using 3D printing technology reduced labor costs by 50 to 8 percent and construction waste by 30 to 60 percent (Carolo, 2020). Figure 2-17, demonstrates the 3D- printed office form outside and inside.

In 2017, University of Nantes in France developed and built what is called Yhnova House in collaboration with Nantes Digital Sciences Laboratory (LS2N) as part of Nantes Design week in 2017. It was built using the university's own patented technology known as Batiprint. The total area of Yhnova House is about 95 square meter and it took 54 hours to 3D print. Figure 2-18, demonstrates Yhnova house from outside.

In 2019, ICON company in collaboration with non- profit organization in Tabasco, Mexico, they built affordable houses for those who ae in dire need. The basic layout includes two bedrooms, a bathroom, kitchen, and living space. Figure 2-19, shows a sample of an affordable house. The project aims to build more than 50 homes (Carolo, 2020).

(a)

(b)

Figure2-17, Office of Future in UAE, 2016 a)- Exterior design. b)- Interior design of OOF (Carolo, 2020).

Figure2-18, Yhnova house, Printed by University of Nantes, France, 2017 (Carolo, 2020).

Figure2-19, Affordable house by ICON and Non-Profit organization, Tabasco, Mexico, 2019 (Carolo, 2020).

In 2019, another record-breaking project was built by Apis Cor, this project for the Municipality of Dubai is the largest 3D printed building to date. The total area of two story is 650 square meter. The main goals of the project were to test the equipment under harsh climate conditions, developing the 3D printing material and construction technologies, and testing the equipment during a long period (Carolo, 2020). Figure 2-20, demonstrates the Municipality of Dubai while it was under and after construction.

(a) (b)

Figure2-20, Municipality of Dubai a)- Under construction b)- After Construction (Carolo, 2020).

In 2020, ICON firm has built about 400 square foot of affordable houses for homeless families in Austin, Texas. For this project, a total of six 3D printed houses were built in cooperation with Logan Architecture. Each structure has a full kitchen, living room, single bedroom, and one bathroom. Figure2-21, demonstrates one of those affordable house.

Figure2-21, 3D Printed affordable houses for homeless by ICON, Austin, Texas

Review of these projects shows that construction industry has been trying to adopt the 3D Concrete Printing (3DCP) technology. There has been an uptick in this trend in the past few years as indicated by the aforementioned examples. It should be, however, noted that almost all these construction examples still utilize some form work and are not fully automated. This is especially a drawback for printing cantilever elements, wall openings for windows, doors, and utility ducts, as well as roofing structurers.

2.5 3D-Printed Concrete for Construction Purposes

Given the nature of 3DPC, the concrete material used for this application must meet certain rheological requirements in order to be successfully used in digital construction of structural elements (Zhu, et al., 2019). Primarily, the fresh concrete mix must be extrudable through the nozzle without agglomerating or clogging the delivery system, which is represented in Figure 2-22, (Ph, et al., 2016). Therefore, the aggregate size, and any other materials extruded, must be relatively fine which places the printable concrete materials more on the concrete mortar spectrum (Ozalp & Yilmaz, 2020) .

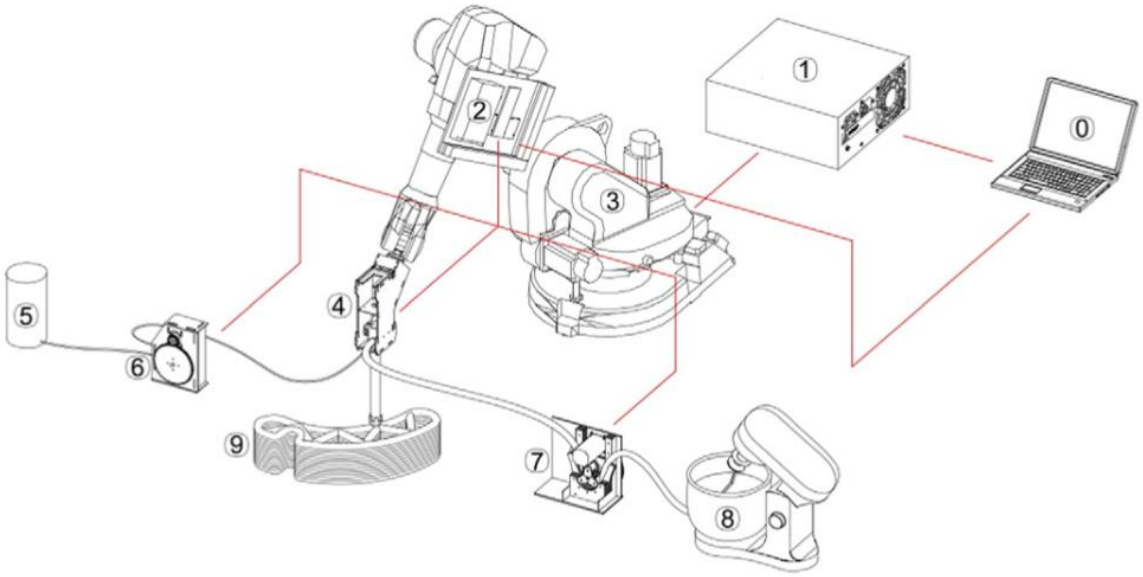

Figure2-22, Schematic of 3D- Printer (Ph, et al., 2016).

2.5.1 Fresh Properties of 3D-Printed Concrete

Using concrete as a construction material with 3DCP technology can pose some challenges, as the fresh properties of the concrete and their evolution with time become highly important. The most predominant properties of fresh 3D printed concrete are shown to be extrudability and buildability, which have mutual relationships with workability and open time window. These properties are significantly influenced by the mix proportions, the presence of rheology modifying admixtures such as superplasticizers, retarders, accelerators and other additives (Le, et al., 2012). These properties are further discussed below:

2.5.1.1 Extrudability *Property*

Extrudability is defined as the ability to transport the fresh concrete material through a hopper and pumping system to a nozzle, where it must be extruded as a continuous filament (Le, et al., 2012) (Guowei, Junfei, Li, Zhijian, & Junbo, 2018). The Extrudability of 3D-printed concrete evaluation could be done using either the visual inspection or digital evaluation methods. To visually determine the extrudability, several single layers can be printed with certain length. Any occurring blockage and/or tearing/fracturing will be identified through visual inspection (Le, et al., 2012) (Guowei, Junfei, Li, Zhijian, & Junbo, 2018). Furthermore, another visual assessment method, called Print Quality, was proposed by the researchers from the University of Southern California, where the printed layers are visually tested for surface defects, inadequate cohesion, rounded edges and changes in dimensions (Kaszyńska, Hoffmann, Skibicki, & Zieliński, 2018). Fig 2-23 and Figure 2-24, show the evaluation of extrudability using visualization method.

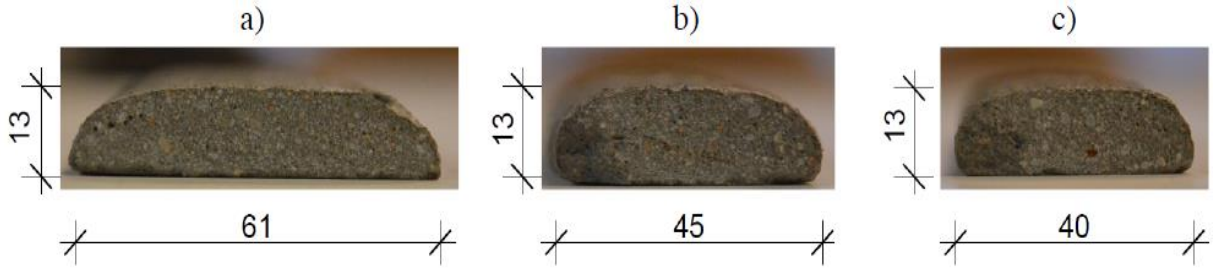

Figure2-23, The influence of Pump output on layer dimensions.
a)- output of 2.88 l/min, b)- output of 2.12 l/min, c)- output of 1.33 l/min (Kaszyńska, Hoffmann, Skibicki, & Zieliński, 2018)

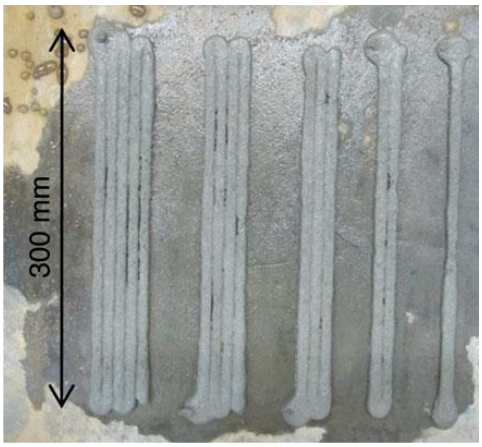

Figure2-24, Test sample to evaluate the Extrudability property (Le, et al., 2012)

On the other hand, digital evaluation is done using a viscometer, see Figure 2-25. A viscometer is a digital device that can serve as an indicator of variations in extrudability on the basis of the static, dynamic yield stress, and shear stress (Nerella, Näther, Iqbal, Butler, & Mechtcherine, 2018). In addition, van shear apparatus was used to determine the applied torques and the shear stresses of fresh concrete (Le, et al., 2012). Le and his team found that the values of shear strength to have a printable mix should range from 0.3 to 0.9 kPa as it can be noticed from Figure 2-26, which demonstrated the values of shear strength for the same water binder content with different dosages of superplasticizer.

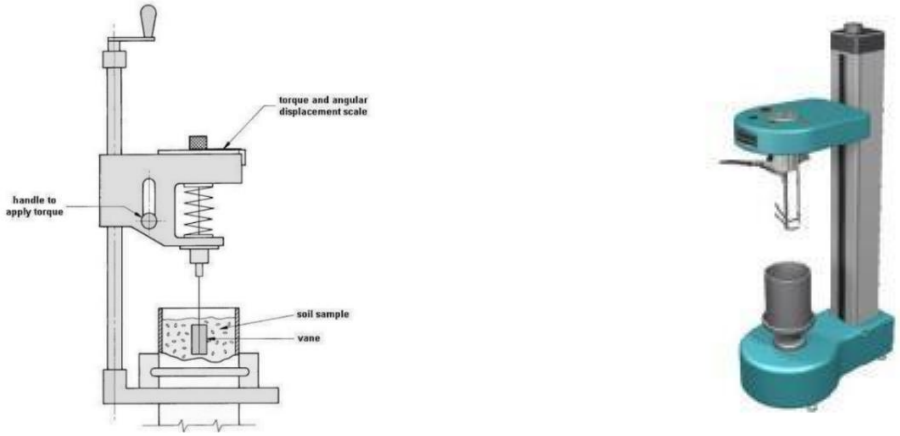

Figure2-25, a)- Van shear apparatus b)- Viscometer (Le, et al., 2012) (Nerella, Näther, Iqbal, Butler, & Mechtcherine, 2018)

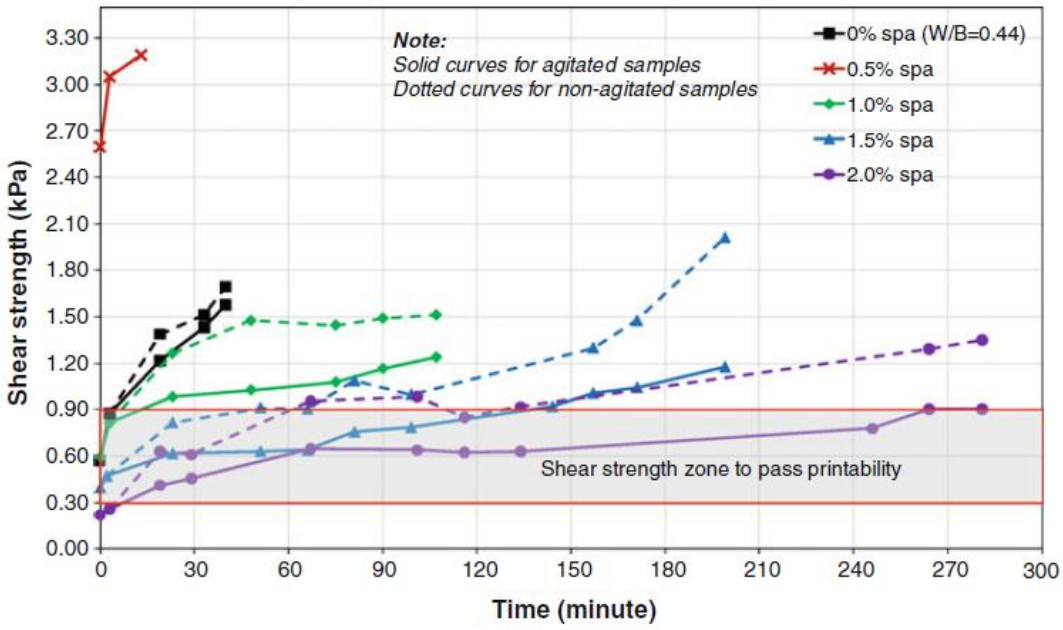

Figure2-26, Shear Strength as an indicator of printability (Le, et al., 2012)

Several factors can affect the efficiency and quality of extrusion such as: 1) Robot speed, discharging capacity of the pump, and the Auger delivery method (Shakor, Renneberg, Nejadi, & Paul, 2017); 2) Combination of practical sizes and the ratio of plasticizer (Le, et al., 2012); and 3) shear strength of the mix.

2.5.1.2 Workability Property

Workability is generally defined as the amount of energy required to achieve the desired level of compaction. It is also defined as the relative ease with which concrete can be mixed, transported, molded and compacted. Similar to extrudability, workability could also be measured through visual and digital evaluation techniques. The well- known slump test, for instance, is an empirical-based visual method. In case of 3D –Printed fresh concrete the desirable value of slump ranges between 1 to 3 mm (Paul, Tay, Panda, & Tan, 2018) in order to avoid any significant deformation in the printed layers. In other words, a 3D printable mix needs to have a negligible slump value. However, given the nature of printable concrete mixes, traditional slump test might not be the best candidate to evaluate the workability. On the other hand, digital evaluation can also

be performed using viscometer which can evaluate the workability and its evolution at different time intervals (Le, et al., 2012).

The workability is significantly influenced by the presence of superplasticizer, retarder and accelerator in a mix. Dosages of any of these admixtures should be further calibrated and verified with extrusion pump capacity. Some researchers recommend that the initial amount of superplasticizer admixture can be assumed as a percentage of the binder content and should be calibrated based on the shear strength of a mix in order to achieve the desired values that were mentioned earlier in this section. Figure 2-27, Figure 2-28, and Figure 2-29, show the effect of using plasticizer, accelerators and retarder on the mix workability, respectively (Le, et al., 2012).

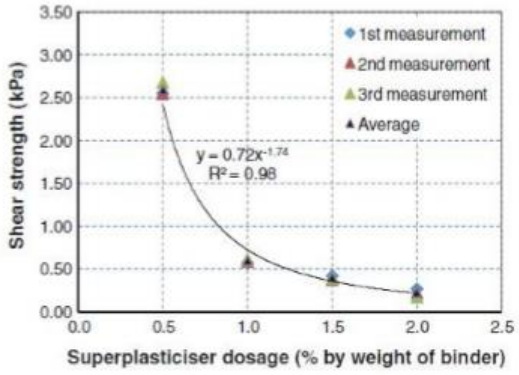

Figure2-27, Effect of plasticizer on shear strength of fresh concrete mix (Le, et al., 2012).

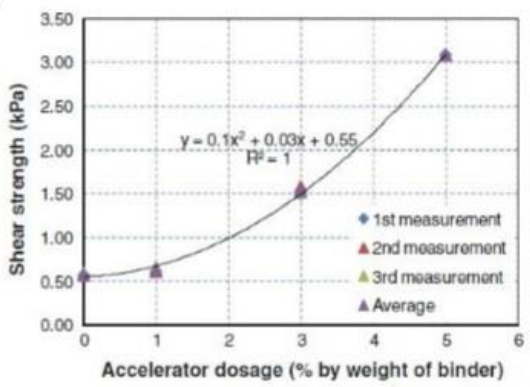

Figure2-28, Effect of accelerator on shear strength of fresh concrete (Le, et al., 2012).

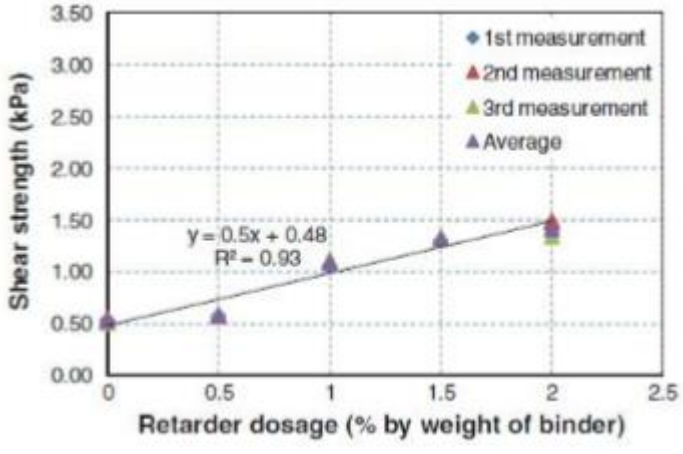

Figure2-29, Effect of retarder on shear strength of fresh concrete mix (Le, et al., 2012).

2.5.1.3 Buildability Property

Although workability and extrudability are essential parameters, 3DCP cannot become feasible without accounting for the desired level of buildability, which is an important parameter of printed layers. Buildability determines the feasibility of stacking a freshly extruded mix layer by layer and its resistance to deformation under the pressure of the subsequent layers (Pan, Jiang, He, Wang, & Yin, 2020). Balancing the printability and buildability has been known as one of the most critical optimization problems in this area. This is because several factors can have a significant contribution to the rheology of the fresh mortar, and hence multiple combinations of these parameters can be feasible to come up with the right printable mix that achieves the higher buildability. These factors significantly influence the adhesion efficiency between the printed layers that affect the bond strength (Al Jassmi, Al Najjar, & Mourad, 2018).

Buildability property could be evaluated using either the empirical methods or the mechanistic digital methods. Using the digital evaluation, such as squeeze flow test is more preferable in order to reduce the amount of wasted materials to test the buildability of each mix. This method becomes more important, especially if there are many mixes which need to be tested. The empirical/visual evaluation is done by counting the number of subsequent layers that could be stacked on the top of each other before the assembly collapses, and also checking whether there is a significant deformations in the underlying layers as shown Figure 2-30. This method, however, cannot provide a mechanistic evaluation of the buildability characteristic for fresh concrete mixes while it requires much more materials (Le, et al., 2012).

Figure2-30, Visual evaluation of Buildability Property (Le, et al., 2012)

To create more meaningful data regarding the structural capacity of stacked layers of fresh concrete, different compression and shear tests have been proposed in the literature. For example, the squeeze flow test was used to determine the strain under compressive load (Shakor, Renneberg, Nejadi, & Paul, 2017). The squeeze flow test is oriented towards Brazilian standard testing method ABNT NBR 15839:2010 (Shakor, Renneberg, Nejadi, & Paul, 2017) and subjects the specimens to different types of stress/stains as illustrated in Figure 2-31. Where No.1 represents the top plate with a diameter of 101 mm and surface roughness Ra0.0586, No.2 represents mold ring with the same diameter as the former, No.3 represents the mortar sample, and No.4 represents the bottom plate with a dimeter of 160 mm and surface roughness Ra0.0586. The test can be performed using a conventional compressive testing machine. The displacement speed is approximately 0.1 mm/second. The roughness of the contact areas adjusts the major mechanisms to be shear stress or elongation. This test can help determine the vertical and horizontal strain of bottom layers subjected to vertical compressive load from overlaying layers. Through the use of a dynamic pressure system, 3D visualisations of pressure distribution in the samples can be rendered to detect stress peaks in the specimen or even in printed filaments with some modification to the setup .

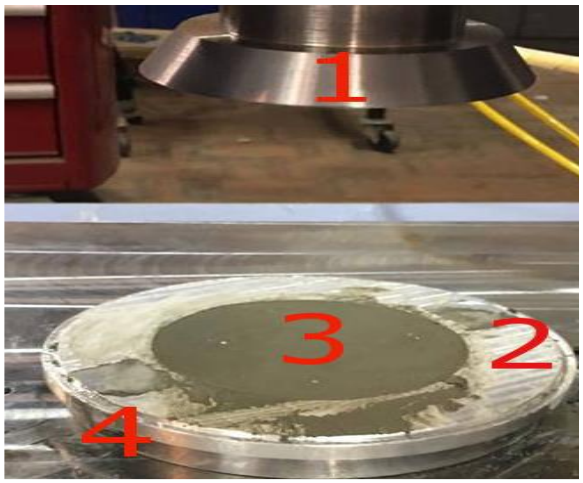

Figure2-31, squeeze-flow (Shakor, Renneberg, Nejadi, & Paul, 2017)

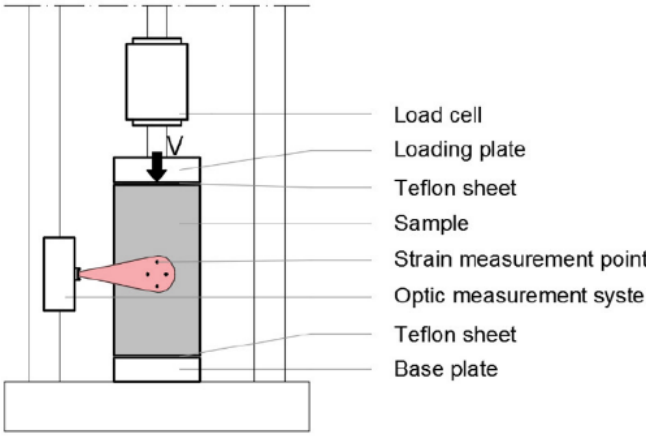

Figure2-32, Cylinder compression test with optic measurement system extrusion (Wolfs, Bos, & Salet, 2018).

The University of Eindhoven uses a similar approach to create compressive strength data of a 3D-printing mix. A cylinder of 70 mm diameter and 140 mm height shall eliminate the size effects of the aggregate particles. The compressive test for this purpose is conducted under displacement-controlled mode with a rate of 30 mm/min continued up to 25% strain level. Because of the large displacements, strains can be better measured with an optical measurement system as shown in Figure 2-32. In order to understand the trend of changes in stiffness with time, compression tests can be performed at 15, 30, 60 and 90 minutes after extrusion (Wolfs, Bos, & Salet, 2018). This could be, especially important for 3D printed structures because the filaments are expected to be self-sustaining upon extrusion, eliminating the need to have any sort of formwork.

The buildability of fresh concrete depends on the level of workability and open time of fresh concrete. Many factors could affect the buildability of fresh concrete some of these factors are briefly discussed below:

Superplasticizer dosage*:* Using high amounts of superplasticizer would result in excessive deformation in layers; therefore, a reduction of the buildability (Le, et al., 2012). This should, however, be looked at with the overall construction scheme in mind and in light of several other factors. In other words, printing a larger structure versus a smaller layout would demand different open time windows and consequently altering the optimum superplasticizer content.

Yield stress: High yield stress of concrete is preferable for better buildability, but too high values can impair the pumpability (Nerella, Näther, Iqbal, Butler, & Mechtcherine, 2018). This can be adjusted depending on the printing equipment to be closer to the lower- or higher-end of the recommended range for a printable concrete mix.

Printing pattern and time gap: Increasing the time gap between layers could lead to decrease the bonding strength which can have a negative impact on the buildability of fresh concrete as reported by (Le, et al., 2012) (Nerella, Näther, Iqbal, Butler, & Mechtcherine, 2018). Therefore, the printing pattern and starting point should be carefully planned before the printing process begins, since it can affect the mechanical performance of the hardened 3D printed concrete. This printing start point can be set in the slicing software to optimize the printing speed, in order to minimize the printing time gap (Jeong, et al., 2019). Figure 2-33, shows an optimization method to control the printing time gap. Ideally, the time gap should be determined in a way that the stacking of individual layer exhibits a minimal or negligible effect on the printed structure, leading to a monolithic-like product.

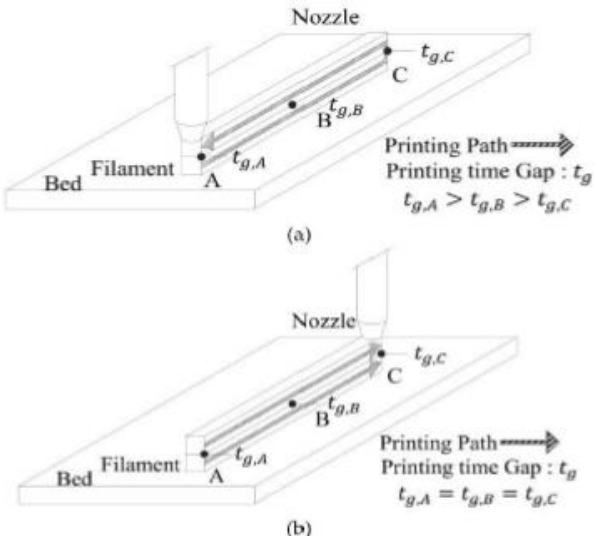

Figure2-33, Classification of printing start point at each layer. (a) Optimized printing start points for fastest printing speed; (b) Selected printing start points closest to specific location (Jeong, et al., 2019).

2.5.1.4 Open Time Property

Different definitions are presented in the literature regarding the open time of fresh concrete materials. According to (Le, et al., 2012), it begins when the workability of fresh concrete

is at a level that maintains extrudability, where the ending of open time can be marked once the shear strength increases by 0.3 kPa from its initial value. According to (Paul, Tay, Panda, & Tan, 2018), open time property of fresh concrete is the time from the moment water was added to the mix until the materials were difficult to pass through the hosepipe to the nozzle during the pumping process (Kaszyńska, Hoffmann, Skibicki, & Zieliński, 2018). The open time is also known as the printability window, which is a period in which the mix maintains proper pumpability.

According to (Al Jassmi, Al Najjar, & Mourad, 2018), balancing the printability and buildability still remains as the most critical aspect of the 3DCP mix design. This is because the adhesion between layers which affects the bond strength, is a function of the time interval between layers. Hence, the process should be designed in a way that the individual layers are able to adhere with one another (an open time that is short enough), and yet, which still have time to cure (an open time that is long enough). This can be done by calibrating input parameters, including: the rate of extrusion, the thickness of layers, linear speed, part cross section, number of layers and the output parameters, including: layer width, part height, vertical profile and surface roughness, (Kaszyńska, Hoffmann, Skibicki, & Zieliński, 2018) and (Nerella, Näther, Iqbal, Butler, & Mechtcherine, 2018).

The open time is defined based on the shear stress test according to the specifications outlined in British BS1377-9:1990 and German DIN 398 (Le, et al., 2012). The research team proposed to test the open time with the V-Funnel method, Vicat apparatus, flow table, penetration tests and mini-cone slump test (Guowei, Junfei, Li, Zhijian, & Junbo, 2018). The predominant factors that can affect the open time of fresh concrete are the amount of superplasticizer and retarder. According to (Le, et al., 2012), superplasticizer has no significant effect on extending the open time, unless it is used at a high rate, which could lead to a negative impact on the buildability (e.g., overly deformed layers). While concurrent use of the retarder and superplasticizer can lead to a reduced demand for the superplasticizer and extending the time window. Figure 2-34, shows the effect of using retarder on the open time property along with using 1% of superplasticizer.

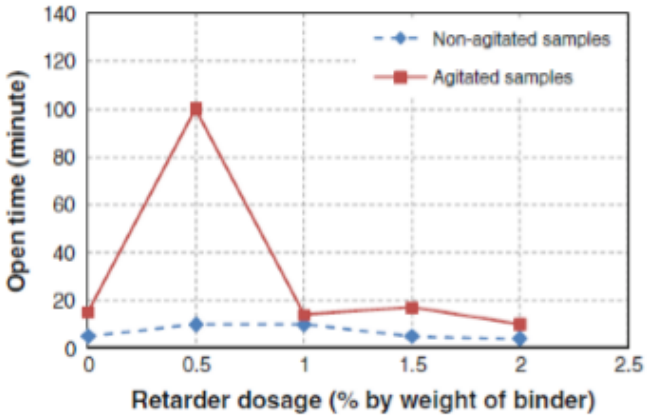

Figure2-34, Open time with different ratios of retarder and 1% of superplasticizer (Le, et al., 2012)

2.5.2 Hardened Properties of 3DPC

More recently and in light of the urge to develop structural specifications, researchers have been shifting their focus on further investigating the hardened properties of 3D- Printed concrete materials, instead of solely focusing on the rheological requirements for controlling the process of printing. However, such studies are still limited in numbers and the evaluation procedures are found to vary significantly from one study to another due to the lack of and existing specification for testing printed specimens.

For example, (Le, et al., 2012) showed that the mechanical behavior of 3DCP can be anisotropic depending on the load directions. In their study, compressive and flexural strengths were evaluated in different loading directions and then compared with cast specimens. The cast specimens had high compressive and flexural strengths about 107 N/mm^2 and 11 N/ mm^2, respectively. On the other hand, the compressive and flexural strengths of printed specimens were lower and varied from 91 to 102 N/mm^2 and 6 to 17 N/mm^2, respectively, depending on the loading directions. Also similar results are observed when comparing the compressive and flexural strengths of 3D-Printed concrete specimens with the cast ones CS by (Panda, Chandra Paul, Jian Hui, Daniel Tay, & Jen Tan, 2017), (Rahul, Santhanam, Meena, & Ghani, 2019) as can be seen in Figure2-36. Figure 2-35, shows the loading directions (i.e., Y=parallel to printing direction, X,Z= perpendicular to the printed cross section) that were applied during the compressive and flexural testing of printed specimens to investigate their directional strength characteristics.

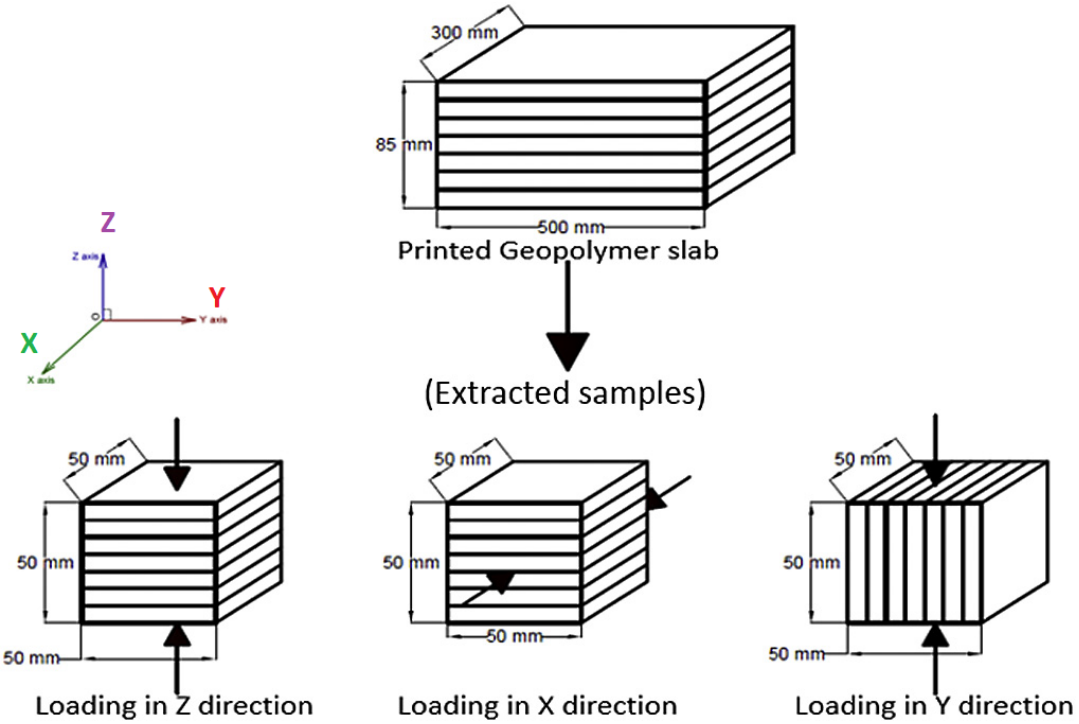

Figure2-35, The testing direction for the mechanical properties (Panda, Chandra Paul, Jian Hui, Daniel Tay, & Jen Tan, 2017).

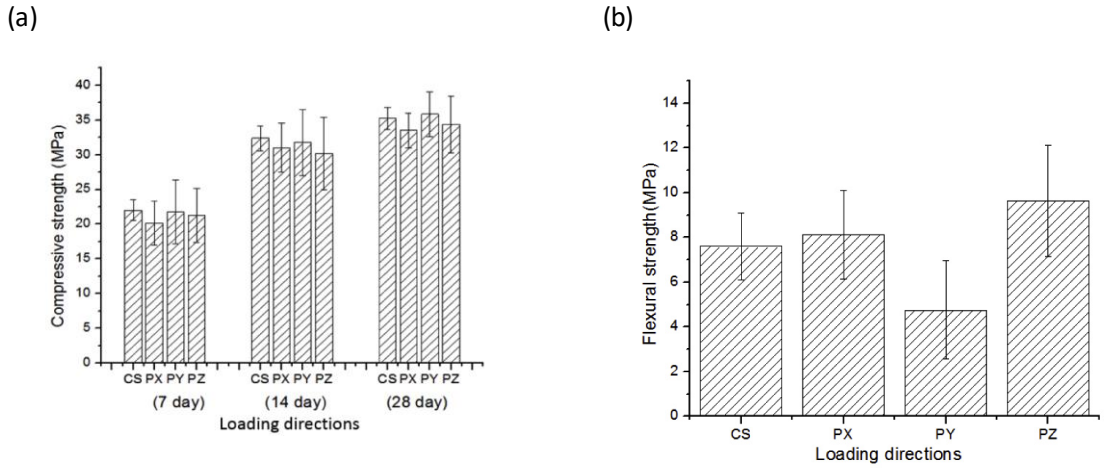

Figure2-36, a) Compressive Strength for cast and printed specimens. b) - Flexural strength for cast and printed specimens. (Panda, Chandra Paul, Jian Hui, Daniel Tay, & Jen Tan, 2017).

On the other hand, the results obtained by (Nerella, Näther, Iqbal, Butler, & Mechtcherine, 2018) found that the compressive strength of printed specimens was higher by 10% as compared to those of the cast specimens. Furthermore, the results that reported by (Zhang, Wang, Donga,

Yu, & Han, 2019) showed nearly equal values of cast and printed specimens. These contradictions in the results imply that there might be other factors that could have affected the mechanical properties of the printed specimens in different ways. Such factors can include the inherent different among different concrete mixes ingredients, the 3D-printer system characteristics, and the quality of printing itself. For instance, the results reported by (Panda, Chandra Paul, Jian Hui, Daniel Tay, & Jen Tan, 2017) showed that the tensile bond strength is highly dependent on the printing parameters, such as the time gap between two printed layers and the height from which the nozzle deposits the layer. It was found that the bond strength decreases with increasing the time gap or an increase in the vertical offset of deposition. Figure 2-37, demonstrates the effect of time gap on the bond strength between the printed layer. The tensile bond strength was conducted in accordance with BS EN 196-1:2016 standard as it can be seen in Figure 2-38. The researchers have agreed that the 3D printing concrete has an anisotropic behavior when it is tested in different directions. However, there are some contradiction regarding the strength when the printed specimens are compared with the cast ones. Some researchers showed that the cast concrete specimens exhibit better compressive and flexural strengths, while other researches have demonstrated the opposite.

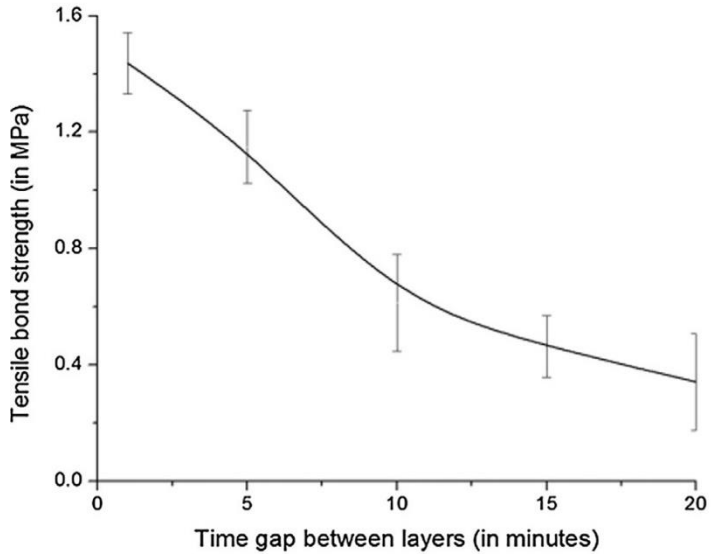

Figure2-37, The effect of time gap on the bond strength (Panda, Chandra Paul, Jian Hui, Daniel Tay, & Jen Tan, 2017)

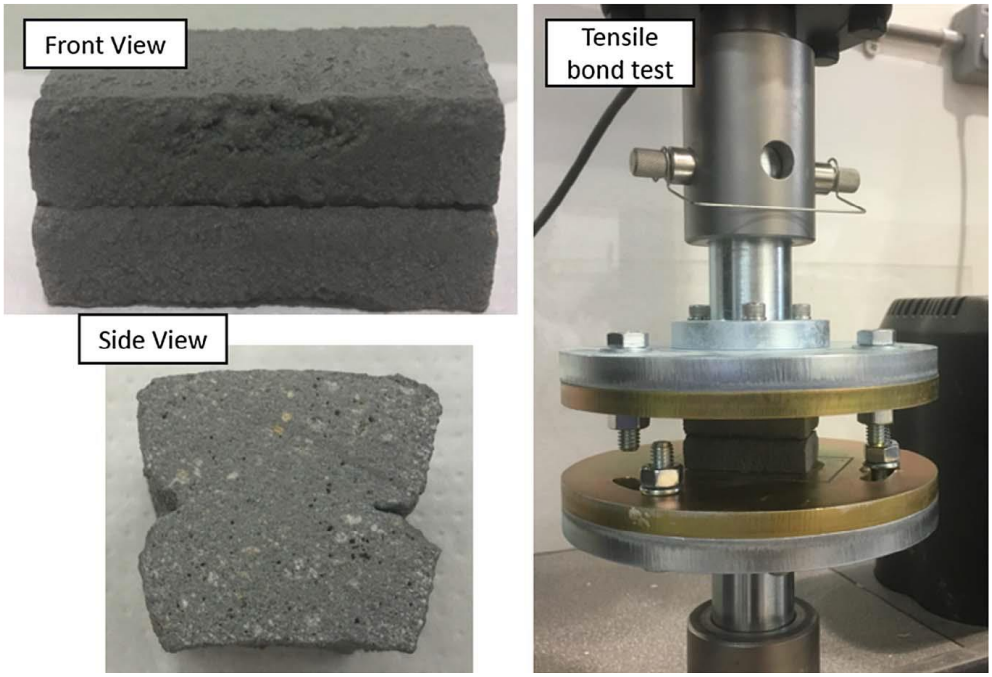

Figure2-38, The tensile bond test (Panda, Chandra Paul, Jian Hui, Daniel Tay, & Jen Tan, 2017)

To this end, contradictory results were reported from different research projects, some of them claim that the mechanical properties of the cast specimens are higher than the printed ones. While the others reported the opposite. In addition, the specimens' dimensions were not big enough to represent properly the effect of bond strength between the printed layers. Thus, one of the objectives of this study is to investigate the mechanical properties of both cast and printed specimens.

Chapter 3: Experimental Program

3.1 Test Methods

Developing high- performance and 3D printable concrete mixes using slag as supplementary cementitious material, has been set as the main goal of this research. The specific objectives were then defined accordingly during the development of the experimental program to achieve this goal. In order to achieve that, several test methods had been adopted from the literature review. An overview of testing methods, parameters, and dimension is given in Table 3- 1. More details about the tests' equipment are provided furthermore in the evaluation sections.

Table 3-1, Test methods and specimens dimensions.

Testing Method		**Investigated Parameter/ Specimens' Dim**	
Fresh Properties	Van shear Apparatus: **BS 1377-9:199**	Shear Strength	300mm*320mm
	Visual Evaluation	Extrudability, Buildability	_____
Hardened Properties	Compression Test: **BS EN 12390-2:2009**	Compressive Strength Cast/ Printed	100*100 mm
	Flexural test: **ASTM C78/C78M- 18**	Flexural Strength Cast/ Printed	100*100*450 mm

3.2 Methodology

An experimental approach has been pursued in this research in order to achieve the goal of the study. A critical review of the literature was conducted at the first stage (Chapter 2), which resulted in gathering the general requirements for 3D printable concrete mixes as well as a baseline for promising trial mix designs. Preliminary candidates for the mix design were evaluated in a sequential manner and adjustments were made to come up with a final mix design that meets the rheological, structural, and logistic requirements. To this end, three main factors were considered and investigated, namely SCM contribution, dry superplasticizer dosage, and water to binder ratio.

The research was executed in three stages after the materials selection process, as illustrated in Figure 3-1. During the first stage, the trial mixes were evaluated using a manual printing procedure, where a frosting bag with a rectangular nozzle was used to extrude the mixes in order to evaluate their printability and buildability. The nozzle in this step has a cross section of 15 mm by 30 mm. Visual evaluation was conducted for both of them. If there is any significant discontinuities or remarkable deformations in the base layers, we drop the mix otherwise it will pass to the next stage, see Figure 3-2. The second stage is the automatic printing; the steps are almost the same as the first stage, except the fully automated system is used to extrude the concrete. Many mixes are expected to pass the visual evaluation so the optimum one will be chosen to move forward to print the wall with it, see Figure 3-2. The third stage then covers the hardened concrete properties and helps comparing the cast and printed specimens in terms of compressive and flexural strengths, see Figure 3-3. In order to keep the scope of the work reasonable, the effect of superplasticizer content on the compressive strength of specimens was first evaluated using cast specimens prior to printing specimens. To this end, the mix with maximum compressive strength at day 7 was selected and the printed specimens were cured for 7 and 28 days before being tested in compression and flexural modes.

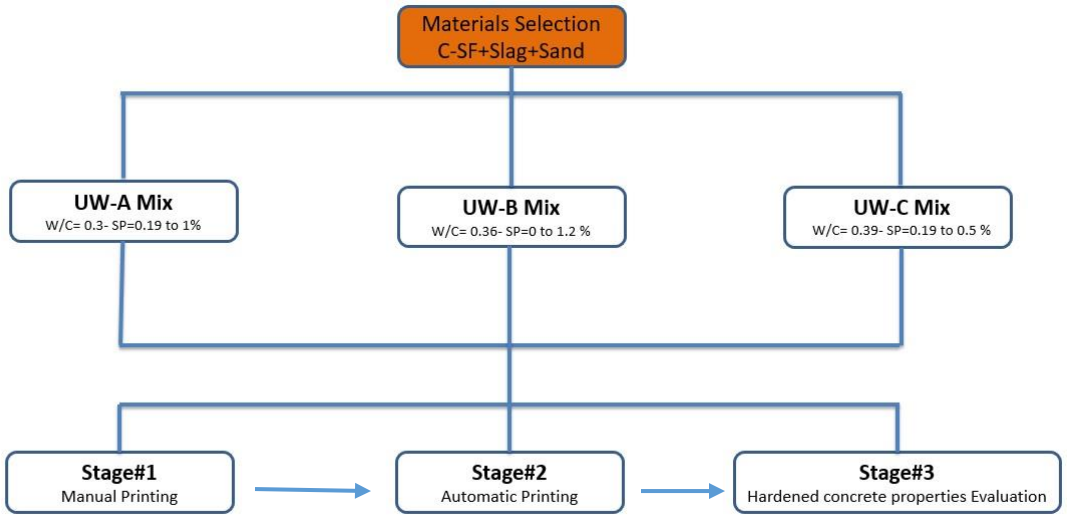

Figure 3-1, Materials selection and research stages

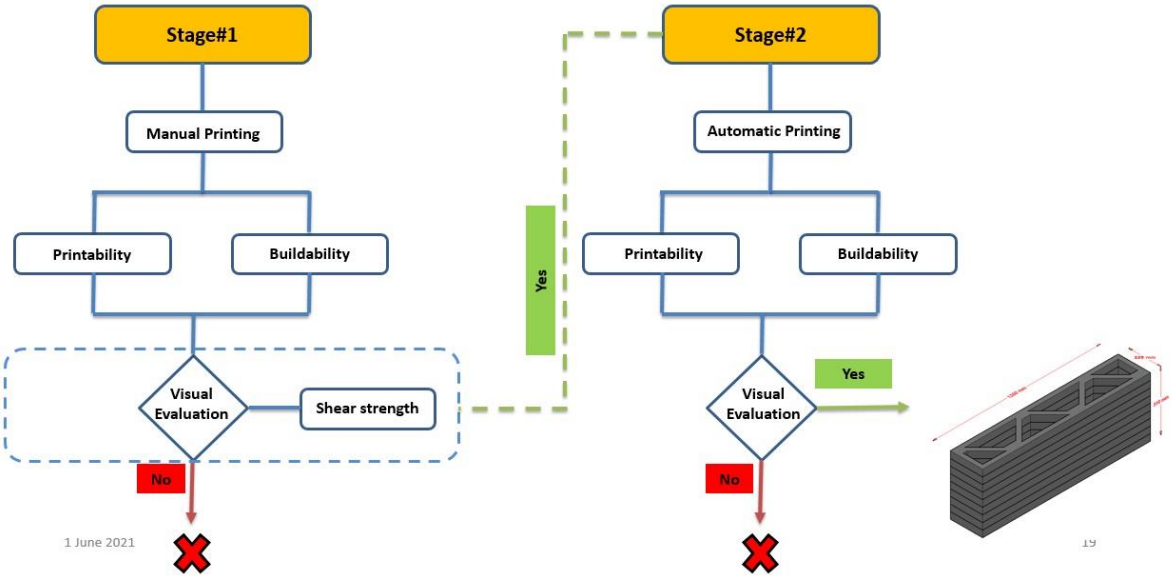

Figure 3-2, Manual and automatic printing stages of the research

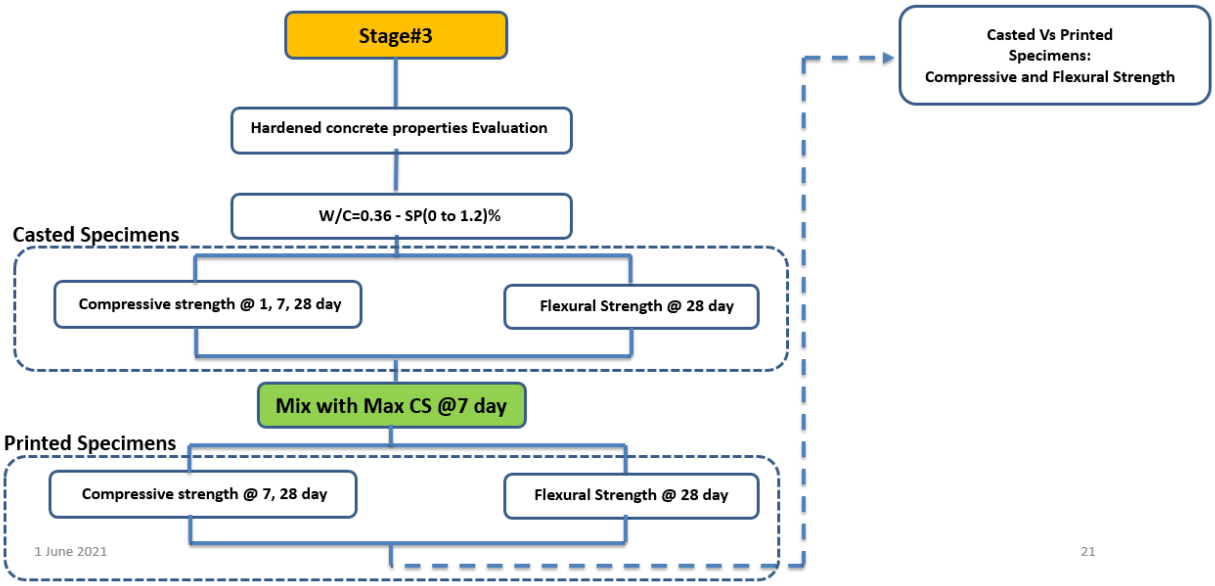

Figure 3-3, Stage three- hardened concrete properties

3.2 Raw Materials

3.2.1 Aggregates

As shown in Figure 3-4, the aggregate gradation used in most of the published work was on the fine-grained spectrum, with many of them following proximity to a packing density to obtain the optimal sand gradation in the mix design. In order to avoid any discrepancies due to the material variability during this study, 18 metric tons of fine-grained sand from a single quarry source in the Region of Waterloo was obtained and stored to be used throughout the course of this project. The particle size distribution for the sand is presented in Figure 3-5 as compared to the upper (UL) - and lower-limit (LL) in Ontario Provincial Standards and Specifications (OPSS). In order to measure the exact water cement ratio, it was necessary to determine the saturated surface dry (SSD) state moisture content of the sand. This moisture level then should be compensated to avoid alteration to water binder content. Therefore, the absorption and the specific gravity tests were conducted in accordance with ASTM C128-15, and the results are presented in Appendix A.

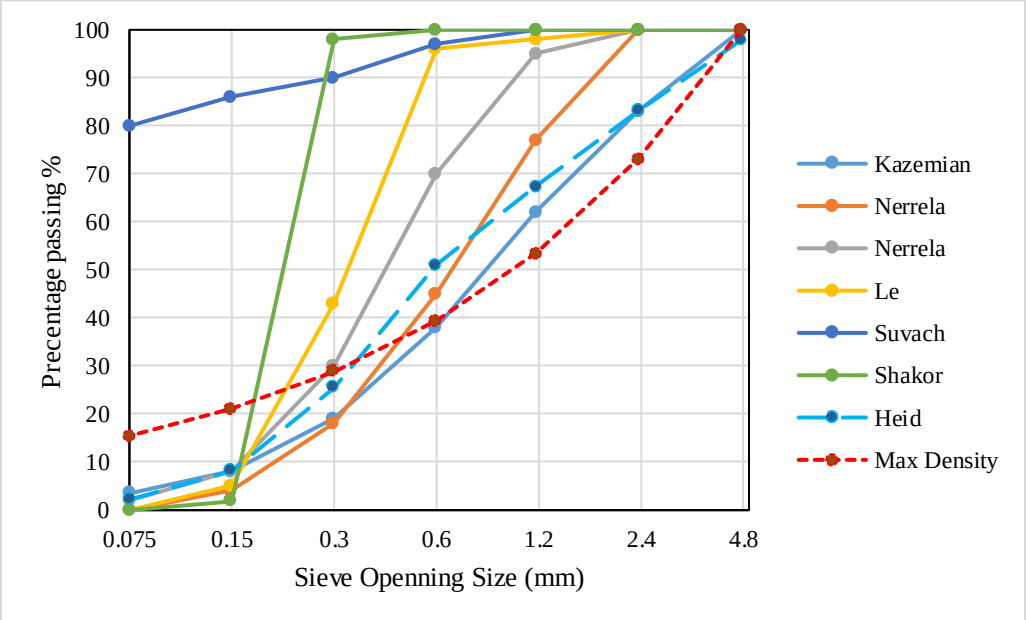

Figure 3-4, sand gradation and packing density curves

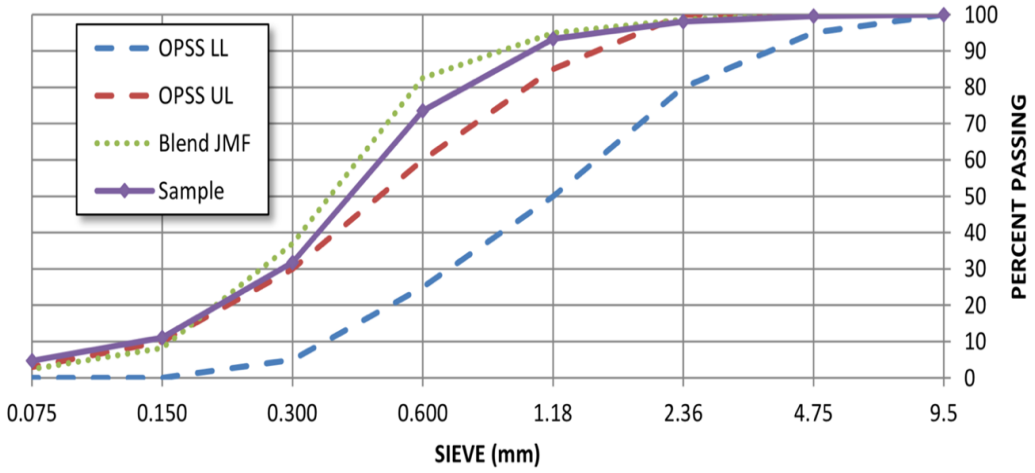

Figure 3-5, particle size distribution of the sand used in this study

3.2.2 Cement (GUb-SF type)

As for the cementitious materials, instead of a general use GU type cement, partial replacement of the cement with supplementary cementitious materials was considered. Such replacement contributes to lowering the generated heat of hydration, lime consumption, forming hydration products, filling the pores and voids, and therefore improving several physical and mechanical properties of the product. To this end, a GUb-SF type cement was selected to be used in this study, where 8% of the total blend is composed of silica fume. The pre-blended silica fume has two immediate benefits one being commercially available, and the other being the homogeneity of the blend. The silica fume contributes to workability of the mix and forming a denser C-S-H gel, which increases the mechanical properties of the concrete mix.

3.2.3 Ground Granulated Blast Furnace Slag (GGBFS)

While use of Fly Ash, especially class C, has been a common practice in the European published work and the United States, absence of domestically produced fly ash was considered a downside for its use in this research. Alternatively, Ground Granulated Blast Furnace Slag (GGBFS), commonly called slag cement, which is a recovered industrial by-product from the iron and steel industry (Slag Cement Association) was considered for the mix design. GGBFS are composed of a mixture of iron oxide, magnesium oxide, and silicon dioxide. The GGBFS used in this research was supplied from Stoney Creek Plant in Ontario, Canada. The benefits of using slag as a cement replacement are the ability to substitute cement content up to 50% while with fly ash

the recommended percentage is 20% % (Thomas, 2007), long term durability, decreased permeability, and increased resistance to alkali silica reaction and sulfate attack (Lafarge, n.d.). Replacement Portland cement with GGBFS ultimately lead to significant improvement in the mechanical behavior but could lead to lower the early strength at early ages (Lim, Hussin, & Ling, 2012). The effect of substituting slag with 40%, 50%, and 65% of Portland cement was investigated by (Hogan & Meusel, 1981), the outcomes of this investigation had shown that the mixes with 40% to 50% of Slag resulted in highest strengths at ages from 28 days to 1 year. Given the recommendation had been provided by the literature review to improve the mechanical properties with using GGBFS and to move forward with economical mix design, 40% of the cement was replaced with slag cement in this study

3.2.4 Superplasticizer

Reducing the water to cementitious binder (W/CM) ratio is common practice, especially in case of high-performance concrete mixes and achieving higher strengths. However, the reduction in w/b will sacrifice the workability of the mix, and hence it needs to be compensated by a water reducer (aka plasticizer) admixture. As for 3DCP application, the required slump test value of fresh concrete should not exceed 2 mm; therefore, the concurrent effect of superplasticizer and water to binder ratio was considered as one of the major tasks in the experimental work in order to improve both the workability of fresh concrete state and the mechanical properties of the hardened material.

Superplasticizers are generally available in liquid and powder forms, with the former being the most common type due to its ease of application in daily production. However, powder form plasticizers are also available and can be highly beneficial for specialty mixes such as printable concrete materials. The printing platform used in this research to produce 3DCP required the use of dry ingredients, including the superplasticizer admixture. Therefore, a powder-based admixture was selected in this research after through consideration of different commercially available options. Details of the UW 3D Printing platform which was developed in collaboration with the Mechanical and Mechatronics Engineering Department is discussed later in this chapter. High range water reducer was used in this research as the superplasticizer because of its compatibility with most admixtures including air entraining agents (in case of future needs), accelerators, and most of the cementitious materials. Different trail mixes were prepared to verify the mix performance.

3.3 Developed 3DCP Platform at the University of Waterloo

A core part of the digital construction is the integrated system that enables automated construction of the structure with minimum human intervention. The system needs to control/adjust the materials mixing, delivery, and automatic deposition as programmed. To this end, an integrated robotic platform was developed at the University of Waterloo in a dedicated 3D Printing Lab (i.e., E3-2139). The developed platform consists of two main zones, mixer and its delivery system, and the robotic arm as shown in Figure 3-6.

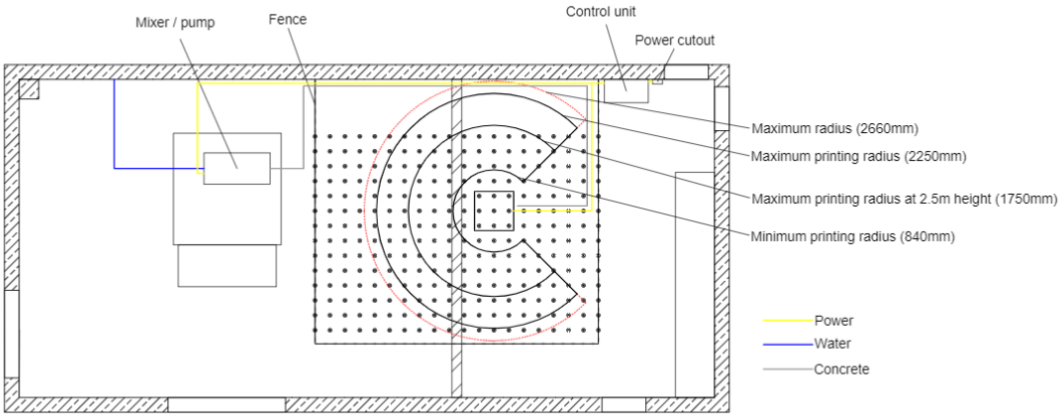

Figure 3-6, 3D- printing platform's layout

Concrete production and its delivery to the robotic arm take place through the use of a combo system which consists of an integrated concrete mixer and pump in a single unit. Using an integrated mixer-pump unit will considerably enhance the flexibility of the printing system and facilitates scaling up the 3DCP of structures from the laboratory scale to the actual construction site level. After conducting a comprehensive survey of the existing equipment, the m-tec Due-mix 2000 was identified as the most suitable unit for the 3DCP application. The decision was based on the continuous delivery of mixed concrete, pumping capacity, minimum and maximum discharge rates, and the ability to increase the capacity for full scale-construction. The concrete delivery system at the University of Waterloo consists of:

- Concrete mixer and pump: Only dry materials can be fed into the hopper of the Due-mix 2000 machine. Water is proportioned using a calibrated pressurized system and will be introduced at the wet mixing tube. The mixing process and accordingly the amount of fresh

concrete material production is automatically adjusted depending on the pump speed and the specific W/CM ratio. The material is mixed and pumped continuously. Figure 3-7, shows a view of the m-tec duo-mix 2000 system and the mixing unit.

(a)

(b)

Figure 3-7, a- M-tec duo –mix 2000, b- mixing and pumping unit

- Hosepipes: two hosepipes with different diameters, namely an ND-25 of 10 m length and an ND-35 with a length of 13.3 m, are attached to the mixer to transport the freshly mixed concrete to the nozzle attached to the tip of the robotic arm where it should be extruded.
- Nozzle: different nozzles with different shapes and dimensions were manufactured and used to extrude the 3D printable concrete mixes. Circular, square, and rectangular cross section nozzles were used to evaluate the printing quality. Figure 3-8, illustrates the nozzles cross section.

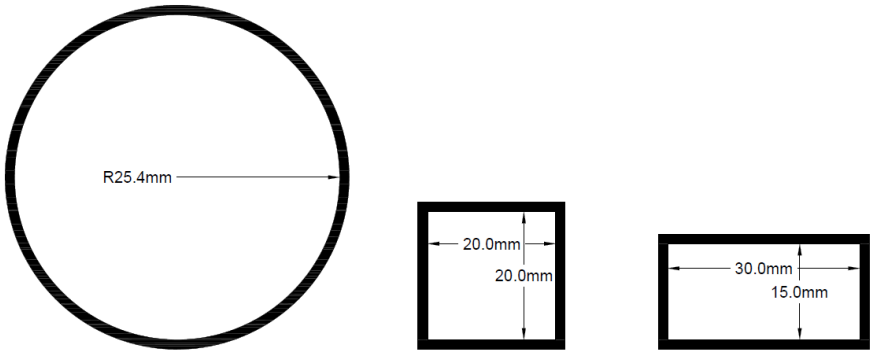

Figure 3-8, Nozzles cross sections evaluated in this research

The nature of 3D- printing projects requires printing flexibility with the capability to adjust the printing speed. As discussed in the Literature Review Section, there are different options for executing the automatic concrete deposition such as CNC machines, gantry type printers, and multi-axis robotic arms. A FANUC R- 2000iA/165F robotic arm with six degrees of freedom was used in this research. FANUC R- 2000iA/ 165F is a floor mounted, versatile arm that has high- performance motion to produce fast cycle times and increase the throughput. It has the capability of handling a variety of applications because of its slim arm that can reach tight spaces, and the six degree of freedom that have been assigned to the printing head. Figure 3-9 and Figure 3-10, illustrate FANUC R- 2000iA/ 165F and robot specification. Figure 3-11, shows the delivery system, robot's arm, and the printing table at the University of Waterloo.

Figure 3-9, Research's robot arm (FANUC R- 2000iA/ 165F)

Robot Specifications		Robot Motion Speed		Robot Motion Range	
Axes:	6	J1	105°/s (1.83 rad/s)	J1	±180°
Payload:	165 kg	J2	105°/s (1.83 rad/s)	J2	+75° - 60°
H-Reach:	2650 mm	J3	105°/s (1.83 rad/s)	J3	+230° - 132°
Repeatability:	±0.2 mm	J4	130°/s (2.27 rad/s)	J4	±360°
Robot Mass:	1210 kg	J5	130°/s (2.27 rad/s)	J5	±125°
Structure:	Articulated	J6	210°/s (3.67 rad/s)	J6	±360°
Mounting:	Floor				

Figure 3-10, FANUC R- 2000iA/ 165F's specifications

Figure 3-11, 3D-Printing lab at UW: a)- FANUC R- 2000iA/ 165F, b)- M-Tec duo-mix 2000

3.4 Mix Design

In order to come up with a printable concrete mix, 12 different mixes, as presented in Table 3-2, were utilized and further evaluated in terms of their printability and buildability properties, with targeted 28-day minimum compressive strengths of 50 MPa. The mixes were broken down under three categories according to water- binder content. The nomenclature WCxSPy was used to refer to the concrete mixes, where x,y represent water/binder ratio and Superplasticizer dose, respectively. The first category was (UW-A Mix), where the W/CM ratio was fixed at 0.30 with

different percentages of the superplasticizer, namely 0.19, 0.5, and 1.00% by weight of the binder content. The second category included (UW-B Mix), where W/CM ratio was fixed at 0.36 with different percentages of the superplasticizer (i.e., 0, 0.19,0.30, 0.5, 0.80, and 1.20% of the binder weight). The third category consisted of (UW- C Mix), where W/CM ratio was fixed at 0.39 with superplasticizer doses of 0.19, 0.25, and 0.50 % by weight of the binder. It should be noted that the recommended dosage of powder superplasticizer would be significantly different from the diluted counterpart made of the same base.

Table 3- 2, 3DPC trial mix designs

Mixes Table [kg/m3] - Mixing time [4 to 6 min]							
Ingrediants	Sand	Gu Cement	Silica Fume	Slag	Water	W/CM	Super Plasticizer
UW-A Mix							
WC0.3 SP0.19	1209	399	35	278	214	0.3	0.19%
WC0.3 SP0.5	1209	399	35	278	214	0.3	0.50%
WC0.3 SP1.0	1209	399	35	278	214	0.3	1.00%
UW-B Mix							
WC0.36 SP0	1209	399	35	278	256	0.36	0.00%
WC0.36 SP0.19	1209	399	35	278	256	0.36	0.19%
WC0.36 SP0.3	1209	399	35	278	256	0.36	0.30%
WC0.36 SP0.5	1209	399	35	278	256	0.36	0.50%
WC0.36 SP0.0.8	1209	399	35	278	256	0.36	0.80%
WC0.36 SP0.1.2	1209	399	35	278	256	0.36	1.20%
UW-C Mix							
WC0.39 SP0.19	1209	399	35	278	278	0.39	0.19%
WC0.39 SP0.25	1209	399	35	278	278	0.39	0.25%
WC0.39 SP0.5	1209	399	35	278	278	0.39	0.50%

The lower-end of the W/CM ratios were limited to 0.30 as theoretically a minimum water to the cementitious materials ratio of 0.30~0.32 is needed for yielding the complete hydration products, otherwise the CM portion will only contribute as a filler in the microstructure of the hardened concrete mix. However, the optimum water content may vary depending on the types of applications and the required workability (Neville, 2010). For instance, in 3DPC application, the

fresh concrete must achieve a certain threshold of workability in order to be extrudable, without sacrificing the buildability property of the fresh concrete (Le, et al., 2012). Therefore, moving forward with minimizing the water content and compensate that with the presence of plasticizer is one of the main objectives in this research.

3.5 Experimental Study

3D-concrete printing research is broken down into three phases at the University of Waterloo, this was started after the materials were researched and selected. The first phase of this research focused on the materials selection and developing 3D- Printable concrete mixes. The first phase is evaluating the printability properties, manually. The second phase is evaluating the selected mixes of the second phase, throughout the fully automated system. In the third phase, the effect of *GGBFS* on the hardened concrete properties was evaluated in addition to determining the mechanical characterizations of cast and printed specimens.

3.5.1 Fresh concrete evaluation

The evaluation of fresh concrete is broken down into two stages. The first one is the manual evaluation, and the second one is evaluation the printability properties of the passed mixes from the first stage the developed 3D- Printing platform at the university of Waterloo.

3.5.1.1 Manual Evaluation Phase

In order to evaluate the trial mixes, and the effect of varying the W/CM ratio along with superplasticizer content on the fresh concrete properties, shear strength of the fresh concrete was used as an indicator, especially to evaluate mixes printability. To this end, a 90 mm diameter vane apparatus was used in this research, because of the relatively low shear strength of the mixes and to avoid the boundary effects, a container with the dimensions detailed in Figure 3-12 was used in all the shear tests. Shear strength was determined from the maximum torque according to BS 1377-9:199 (Le, et al., 2012). Three measurements were taken in three different positions as illustrated in Figure3- 12, and then the average reading was taken. Table 3-3, presents the peak torque values and the calculated shear strength of all the trail mixes in this research. The produced mixes were varied from stiff mixes that could not be evaluated through manual extrusion to very fluid mixes. Therefore, the W/CM ratio was gradually increased to obtain manually printable mixes within the desired range of shear strength. The effect of superplasticizer on the evolution of shear strength on

the three categories of concrete mixes is illustrated in Figure 3-13, Figure 3-14, and Figure 3-15. The observed trend of changes in the shear strength as a function of superplasticizer content was found to be in line with the literature, where there is an indirect exponentially proportional relationship between the strength and the admixture dosage. The shear strength results were then compared to the quality of printability and buildability that were observed during the trial extrusions through a rectangular nozzle of 3 cm by 1.5 cm cross section.

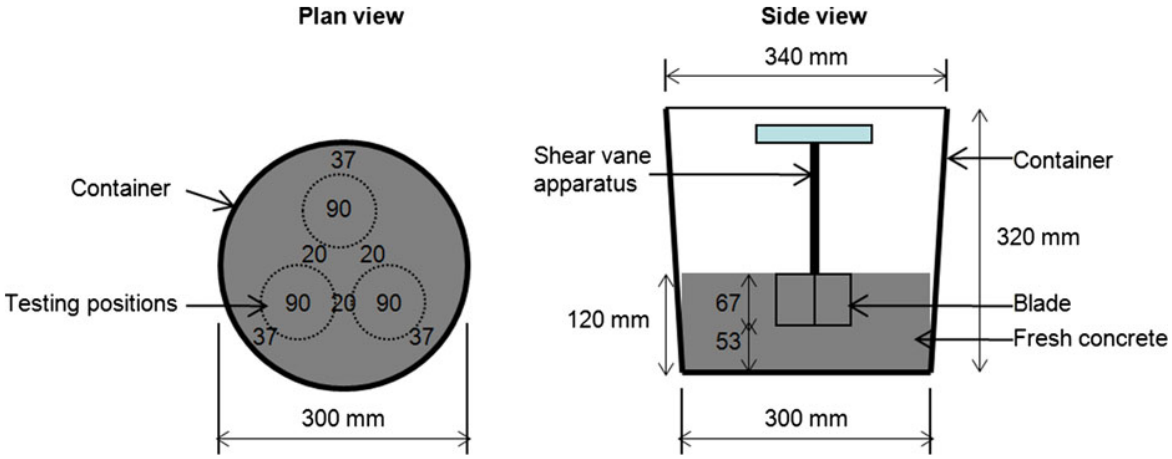

Figure 3-12, Diagram of a shear vane test with measuring positions

Table 3- 3, Maximum applied torque and shear strength of mixes

Mix Name		SP	Applied Torque Kgf.cm	Shear Strength KPa
UW-A Mix	**WC0.30SP0.19**	0.19%	0.05710	1.300
	WC0.30SP0.50	0.50%	0.03995	0.910
	WC0.30SP1.00	1.00%	0.03133	0.710
UW-B Mix	**WC0.36SP0.00**	0.00%	0.01906	0.436
	WC0.36SP0.19	0.19%	0.01567	0.358
	WC0.36SP0.30	0.30%	0.01418	0.324
	WC0.36SP0.35	0.50%	0.01227	0.281
	WC0.36SP0.80	0.80%	0.01044	0.239
	WC0.36SP1.20	1.20%	0.00836	0.191
UW-C Mix	**WC0.39SP0.19**	0.19%	0.01305	0.300
	WC0.39SP0.25	0.25%	0.01044	0.240
	WC0.39SP0.50	0.50%	0.00876	0.190

Such comparison was made to verify the suitability of the recommended range for the shear strength of fresh concrete mixes found in the existing literature and possibly adjusting this range for the type of equipment available at the UW. The first category, UW-A mix exhibited a vey stiff rheological behaviour and could not be properly printed manually. The third category showed a more desirable rheological behaviour that made it possible to manually extrude it for the purpose of printability evaluation. The printed layers by $WC_{0.39}SP_{0.25}$ mix, did not show any discontinuity and expressed a very good buildability without any significant deformations as it can be seen from Figure 3-16. On the other hand, the printed layers using the $WC_{0.39}SP_{0.5}$ mix, exhibited a good printability but suffered from poor buildability as indicated by a significant deformations in the base layer, induced by the weight of the subsequent layers. Figure 3-17, illustrates the deformation of the base layer. The manual printability investigation for the second category of the mixes was postponed due to the lockdown cause by the COVID-19 pandemic in December 2019. Therefore, it was decided to evaluate the printability of this category of mixes directly using the automated system, which happened right after the research team were allowed to return to the campus.

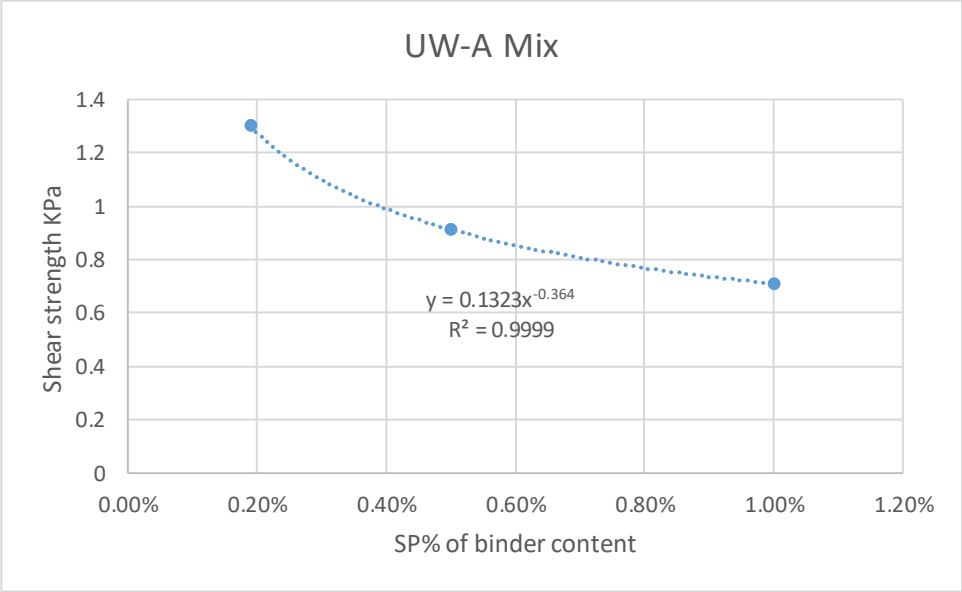

Figure 3-13, Shear Strength's Evolution with Superplasticizer's content

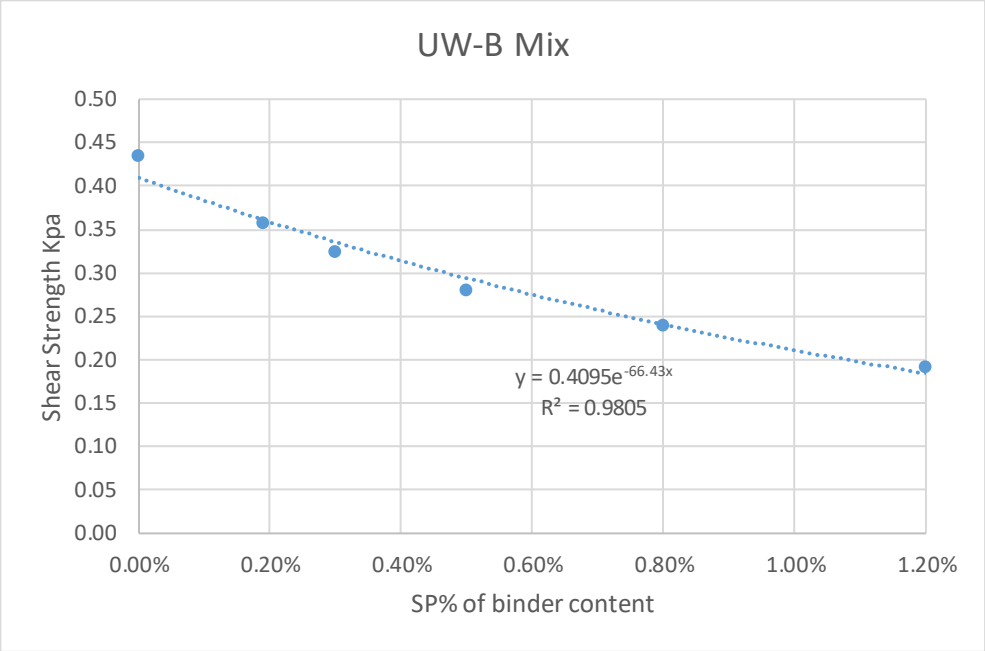

Figure 3-14, Shear Strength's Evolution with Superplasticizer's content

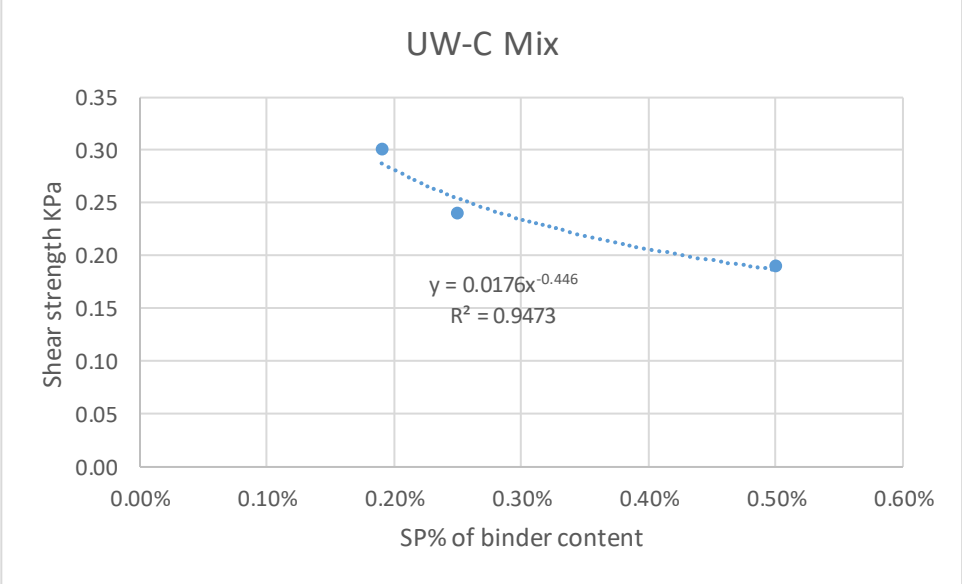

Figure 3-15, Shear Strength's Evolution with Superplasticizer's content

Figure 3-16, manually printed layers using WC0.39SP0.25

Figure 3-17, manually printed layers using WC0.39SP0.5

3.5.1.2 Automatic Evaluation Phase

Next step of the study was focused on evaluating the printability and buildability of the second category (UW-B Mix) and printing a short wall with 45° for the cross patterns inside the wall using the 3DCP platform at the University of Waterloo. Figure 3-18, shows the prototype of the 3D-printed wall using AutoCAD 2018.

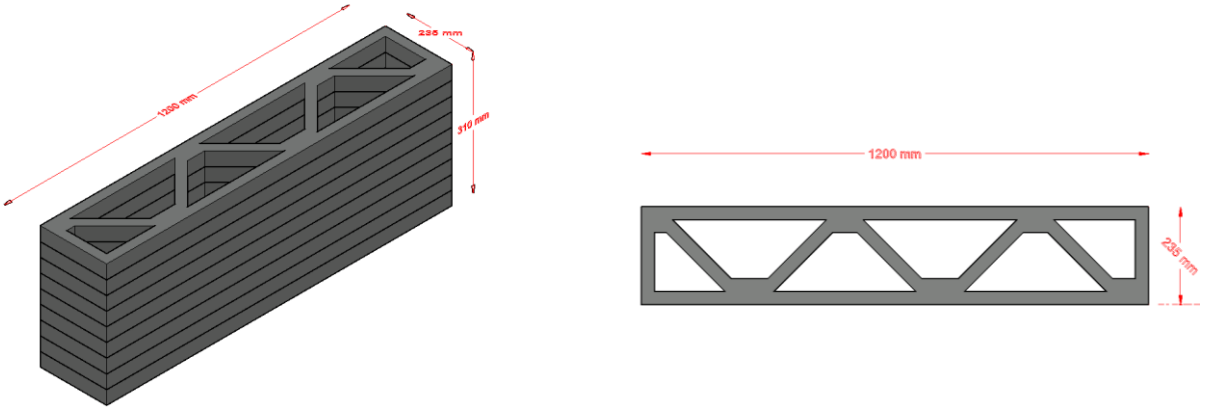

Figure 3-18, prototype of 3D-printed concrete wall for this research

Two printing directions have been set to print the proposed wall, to increase the printing time gap between the start and end points of the printed layers (t= 36.71 sec) and improve the layers buildability. The first direction is assigned to the layers that have odd numbers. While the other direction is assigned to even layers. Figure 3-19, shows the printing directions for odd and even printed layers.

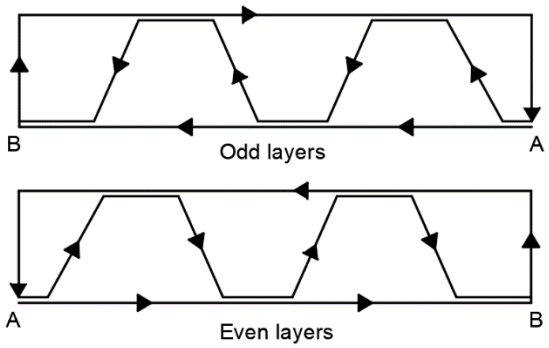

Figure 3-19, Two printing directions for the printed layers

In order to investigate the effect of superplasticizer on the printing quality some robot's parameters were fixed. Table 3-4, demonstrates the fixed robot's parameters.

Table 3- 4, Robot's parameters.

Printing Speed	125-150 mm/sec
Nozzle's height	15 – 30 mm

The first trial was done by using the mix No. (WC0.36SP0.0, SS= 0.436 KPa), the wet chamber clogged because the mix was stiff and could not be easily pumped and that lead to accumulate the materials until it reached the sensor in the wet chamber and stopped the mixer and the pumping system. Figure 3-20 shows the clogging incident that happened due to the materials build up.

Figure 3-20, The clogged wet chamber WC0.36SP0.0

The second trial was done by using the mix No.(WC0.36SP0.19, SS= 0.358 KPa) with a rectangular nozzle (15*30 mm @ 30mm) and the printing speed was 150 mm/sec, the mix was extrudable, but there were significant discontinuities that can be noticed in the printed layers. On the other hand, the mix's buildability did not express any significant deformations, as it can be noticed form Figure 3-21.

Figure 3-21, The printed layers by WC0.36SP0.19

The third trial was done by using the mix No.(WC0.36SP0.3, SS=0.324 KPa) with a circular nozzle (Θ 25.4 mm @ 30mm) and the printing speed was 125 mm/sec. The mix was extrudable and the printed layers showed some discontinuities, and they were dry enough to, significantly, drop the bond strength between the filaments and that did not allow to the printed to stack on top of each other as it can be seen from Figure 3-22.

Figure 3-22, The printed layers by WC0.36SP0.3

The fourth trial was done by using the mix No. (WC0.36SP0.35, SS=0. 281KPa) with a square nozzle (20*20 mm@ 23mm) and the printing speed was set to 125 mm/sec. The fourth mix with SP 0.5% expressed very good printing properties. The printed layers were extrudable without any significant discontinuities and in terms of buildability the printed filaments did not show any remarkable deformations especially in the base layer, therefore, we decided to move forward with printing the proposed prototype. Figure 3-23, illustrates the printed wall (1010*235*315 mm). Figure 3-24, illustrate the printed wall from different views.

Figure 3-23, 3D-Printed wall (1010*235*315 mm) at UW

Figure 3-24, 3D-Printed wall (Top and corners views)

There are a couple of issue were observed during the printing process. Form the printing quality perspective, the fist third of the printed wall (10 cm form the base) expressed very good printability, no discontinuities had been observed in the printed layers, see Figure 3-25. On the other hand, the second third and the last third, the printed layers expressed a good printability but there were discontinuities were observed during the printing. The friction between the stator and its chamber and because of the chemical reaction of silica fume lead to increase the water

temperature and accelerate the setting time of the fresh concrete. Figure 3-26, illustrates the printing quality of the second and last third of the printed wall.

Figure 3 25, the first third of the printed wall

Figure 3-26, the second and the third parts of the printed wall

Regarding the wall's corners, more materials were deposited due to the rotation time that it took to change the printing direction, also the printing speed were dropped from 125 mm/s to zero at the wall's corners which resulted in depositing more materials beyond the printed wall boarders at the wall's corners. The fifth trial were postponed it until we proceed with the third stage and check the effect of superplasticizer on the compressive strength. The mixes that have the highest compressive strength at day 7 will move forward with printing the specimens with it. More details are provided later in the thesis.

3.5.2 Hardened Concrete Evaluation

Studying the mechanical properties of the hardened concrete specimens was carried out under the third stage of this research where the W/CM ratio was fixed at 0.36 and the 3DCP mix design was fine-tuned through investigating the effect of optimum superplasticizer content. Details of these evaluation activities are described in the following sections.

3.5.2.1 Sample preparation

As for testing the hardened concrete, before the cast concrete is scooped into the compressive and flexural molds, the molds were lightly coated in mold release agent; this to ensure that the concrete does not stick to the molds and makes it easier to remove. The concrete samples were scooped into the molds in three equal layers and compacted between each layers, where a hand compaction method was used (Compacting rod in accordance with BS EN 12390-2:2009). The casting and the printing process for the specimens were done in the room temperature with a range of 20 ±5 degrees. Then after 24 hours, the samples were replaced in the curing chamber to ensure a proper hydrate to the printed and cast specimens. To this end, a total of 45 cast specimens were prepared for the compressive strength test in accordance with BS EN 12390-2:2009. Furthermore, 15 prism shaped specimens were casted for the flexural (modulus of rupture) testing in accordance with ASTM C78/C78M- 18. For the printed specimens and due to the limited quantity of the superplasticizer, the number of specimens were brought down to 18 specimens for compressive strength and two specimens for flexural specimens to be tested in two different directions (i.e., Y and Z). Table 3-5, and Table 3-6, present the test matrix for the cast and printed specimens, respectively.

Table 3-5, Test matrix for the cast specimens

Test type	Day	No. Cast specimens					Total Number	Dimension mm		
		SP(0)	SP(0.3)	SP(0.5)	SP(0.8)	SP(1.2)				
Compressive test	1 day	3	3	3	3	3	45	100	100	100
	7 day	3	3	3	3	3		100	100	100
	28 day	3	3	3	3	3		100	100	100
Flexural test	28 day	3	3	3	3	3	15	100	100	450

Table 3- 6, Test matrix for the printed specimens

Test type	Day	No. Printed specimens			Total Number	Dimension mm		
		X	Y	Z				
Compressive test	1 day	3	3	3	27	100	100	100
	7 day	3	3	3		100	100	100
	28 day	3	3	3		100	100	100
Flexural test	28 day	N/A	1	1	2	100	100	450

The cast specimens of stage#3 were prepared by fixing the water to cementitious materials ratio at 0.36 and the superplasticizer dosage was varied from 0 to 1.2 % by weight of the binder. For compressive strength test, the cast specimens were tested at three different ages of 1, 7, and 28-day, while for flexural tests of the cast specimens were tested at 28 day.

The printed specimens were prepared using the superplasticizer content that resulted in the highest compressive strength at 7-day among all the cast mixes. After conducting the compressive test on 7-day cast specimens, the amount of superplasticizer that resulted in the highest compressive strength was determined to be 0.80%. Therefore, the printed specimens were prepared using W/CM of 0.36 and 0.80% superplasticizer content. Regarding the testing procedures, the printed specimens were loaded on different directions to investigate the anisotropic behavior. Figure 3-27, illustrates the established coordinate system for the printed specimens. One of the main purpose of this research is to evaluate the performance of the printed concrete samples versus the cast ones from the compressive strength and flexural strength perspectives.

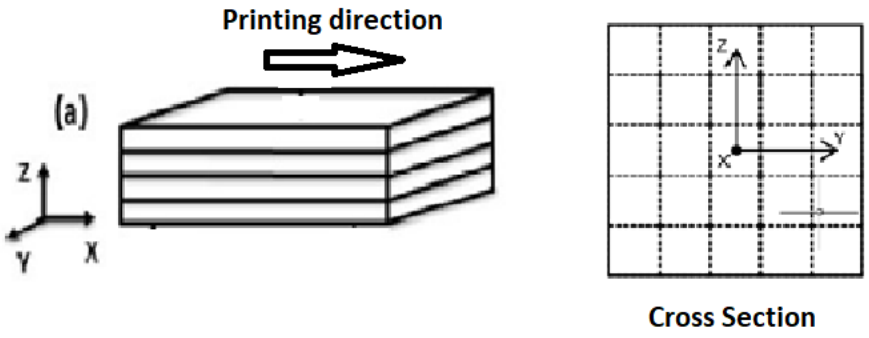

Figure 3-27, The general coordinate system for the printed specimens

3.5.2.2 Compressive Strength Test

The compressive strength test was conducted in accordance with BS EN 12390-2:2009 using an ELE International model #36-3088/02 concrete compression testing machine. A uniaxial load was applied to the cubic specimens with dimensions of 100 by 100 by 100 mm using a loading rate of 2.5 to 3 KN/sec. Figure 3-28, shows the compression testing machine. Given that research on 3D printable concrete mixes is considered relatively new, it is important to have a good understanding about the strain-stress response of the specimens at different ages, rather than solely relying on the peak stress values. Moreover, effect of superplasticizer on the stress – strain behavior of the printed during the compressive strength testing was evaluated during this step. In order to obtain the stress-strain curve, one extensometer with a length of 70 mm was attached to the cube's surface to measure the strain versus the applied load then the data were plotted using Excel 2016.

Figure 3-28, ELE International model #36-3088/02 concrete compression testing machine

3.5.2.2.1 Cast specimens

A total number of 45 specimens were casted and cured for the compressive strength testing. Five different ratios of superplasticizer (e.g., 0, 0.3, 0.5, 0.8, 1.2) % of the binder content were used and tested for three ages (e.g., 1, 7, 28) days and three specimens were assigned for each age.

3.5.2.2.1.1 Compressive Strength at 1-Day Age

Early age compressive strength of 3DCP can be of a high importance as the 3DCP structures are supposed to be self-sustaining without the need to any formwork and molds. Figure 3-29, illustrates the stress- strain curves for specimens with SP contents of (0.3, 0.5, 0.8, and 1.2) % that were tested at 1- Day age. Some testing equipment limitations resulted in not being able to fully capture the stress-strain curve for $WC_{0.36}SP_{0.0}$ specimens due to the limited availability of some materials and the time sensitivity of the tests. Therefore, for the day one specimens containing no superplasticizer, only the peak stress and its corresponding strain were recorded. Furthermore, for the specimens with SP content of 1.2% the applied load rate was slightly higher than the other specimens (i.e., 4.5 to 5 KN/S), because the control unit of the equipment was manually operated. Figure 3-30, shows the ultimate loads and the corresponding strains.

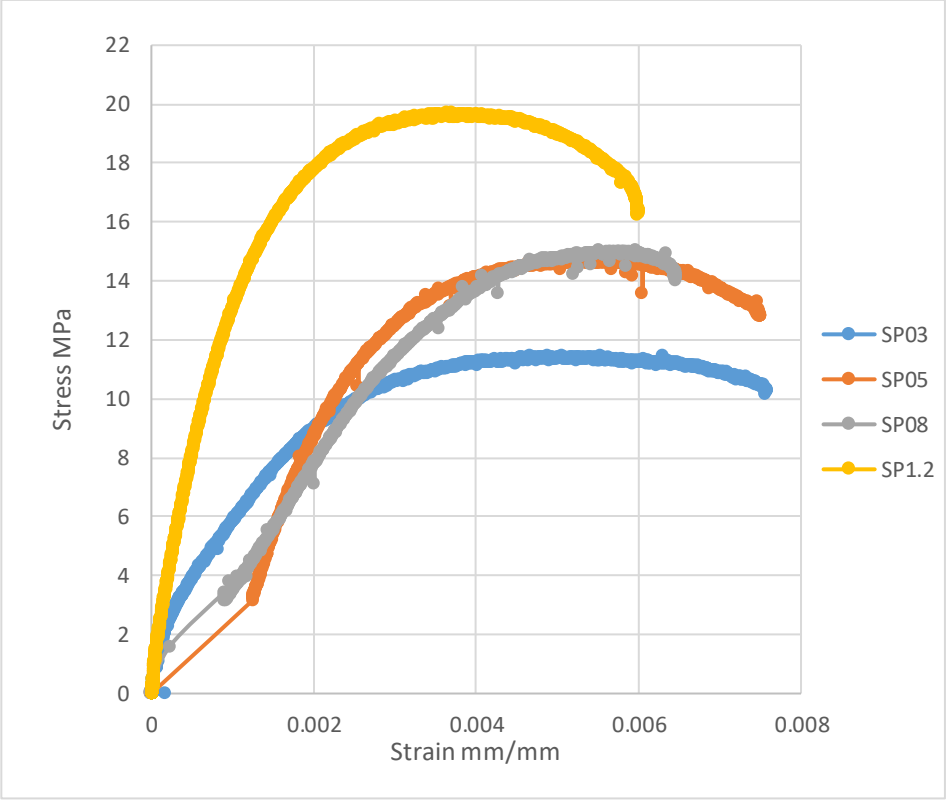

Figure 3-29, Stress – Strain curve at 1- Day age

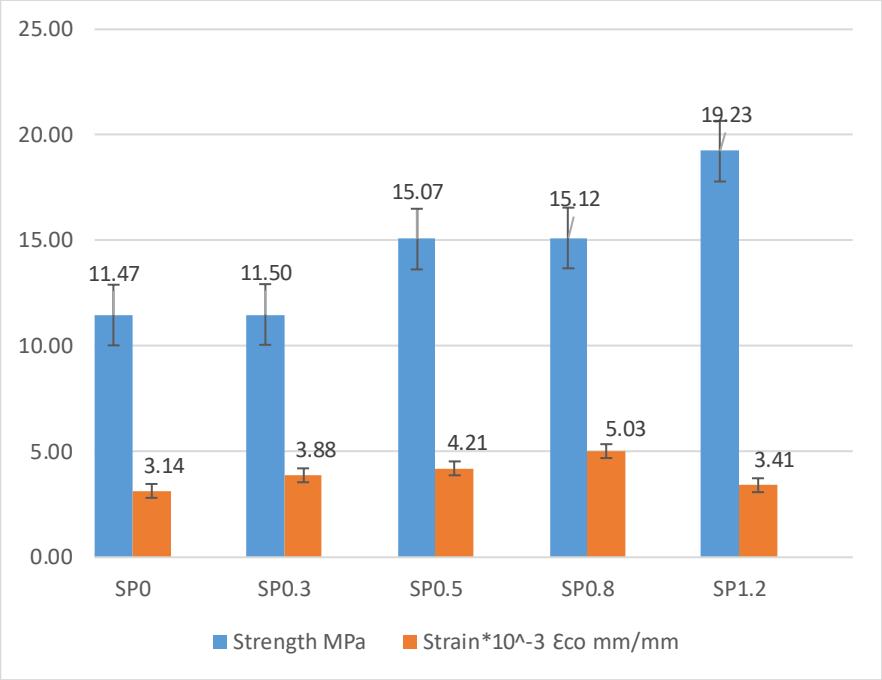

Figure 3-30, Stresses and corresponding Strains at Day 1

$WC_{0.36}SP_{0.30}$ specimens have expressed slightly higher compressive strength than $WC_{0.36}SP_{0.0}$ specimens. On the other hand, $WC_{0.36}SP_{0.5}$ and $WC_{0.36}SP_{0.8}$ specimens have shown higher compressive strength than the former ones. However, WC0.36SP1.20 specimens have expressed the highest compressive strength because the applied load rate was higher than the ones applied on the other specimens as mentioned before. Regarding the corresponding strains to the ultimate loads, it has been noticed that increasing in the superplasticizer contents reflected in higher strains for the same water cement ratio. In consequence, the increase of Superplasticizer's dosage with a given GGBFS ratio, resulted in higher compressive strength because better consolidation is achieved. On the other hand, the effect of superplasticizer on delaying the chemical reactions, which are responsible of hardened the mixes, is noticeable at 1-day age, where the corresponding strains are increased along with increasing the superplasticizer content.

3.5.2.2.1.2 Compressive Strength at 7-Day Age

Figure 3-31, demonstrates the stress- strain curves for the specimens with SP 0, 0.3, 0.5, 0.8, 1.2 % at 7- day age. The compressive strength had peaked with specimens that contained SP (0.8) % with a value of 53.45 MPa, and the corresponding strain was 0.003421. However, the compressive strength has slightly dropped with WC0.36SP1.20 specimens, while the

corresponding strain kept increasing until it reached the value of 0.003601. Figure3-32, illustrates the effect of different ratios of superplasticizer on the compressive stresses and the corresponding strains.

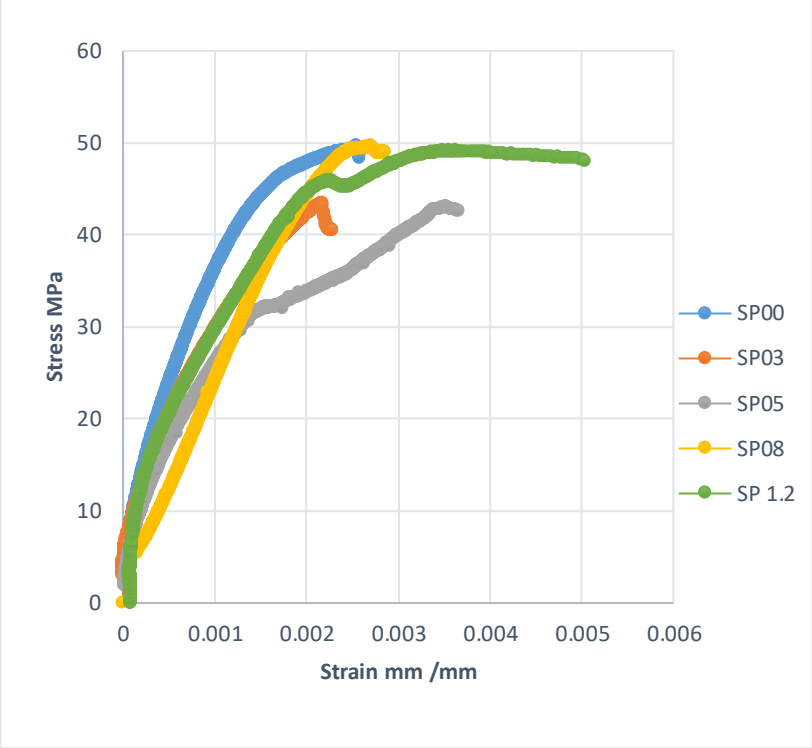

Figure 3-31, Stress – Strain curve at 7-Day age

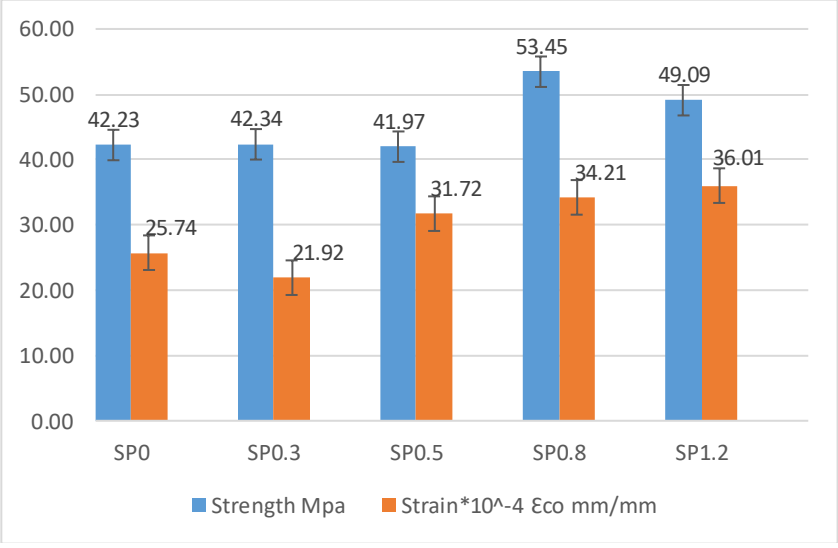

Figure 3-32, Stresses and corresponding Strains at 7-Day age

A significant increase with an average 70% has been noticed on the compressive strength of the cast specimens at Day-7 comparing with the ones at Day-1. on the other hand, the corresponding strains at Day-7 have expressed lower strains comparing with the ones at Day-1.

3.5.2.2.1.3 28-Day Strength Results

Figure 3-33, demonstrates the stress- strain curves for the specimens with SP 0, 0.3, 0.5, 0.8, 1.2 % at day 28. The compressive strength has peaked with specimens that contain SP 0.8, 1.2 % with a value of (71.08, 73.50) MPa, respectively. The corresponding strains were (0.003567, 0.003101) as can be noted from Figure 3-34.

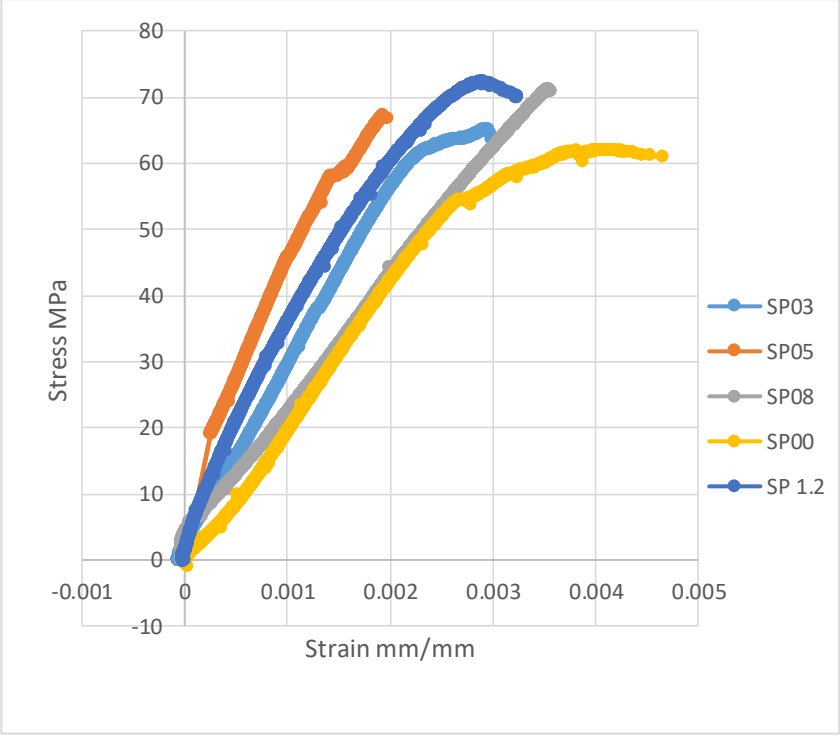

Figure 3-33, Stress – Strain curve at 28- Day age

Comparing these results of day- 28 specimens with the day-7 ones, the compressive strength has increased with an average of 10%. Regarding the modulus of elasticity of concrete, the tangent modulus Ec has been calculated from the stress-strain curves that were obtained from the conducted compressive test. In order to avoid the effect of the fluctuation that comes at the beginning of the test, Ec was calculated starting from 10% to 40% of the ultimate stress. And

then, the experimental tangent modulus of elasticity Eexp was compared with the simplified form that provided in CSA A23.3, Ecal. Figure 3-35, illustrates the evolution of elastic modulus at day 28 along with different superplasticizer contents in comparison with the calculated ones.

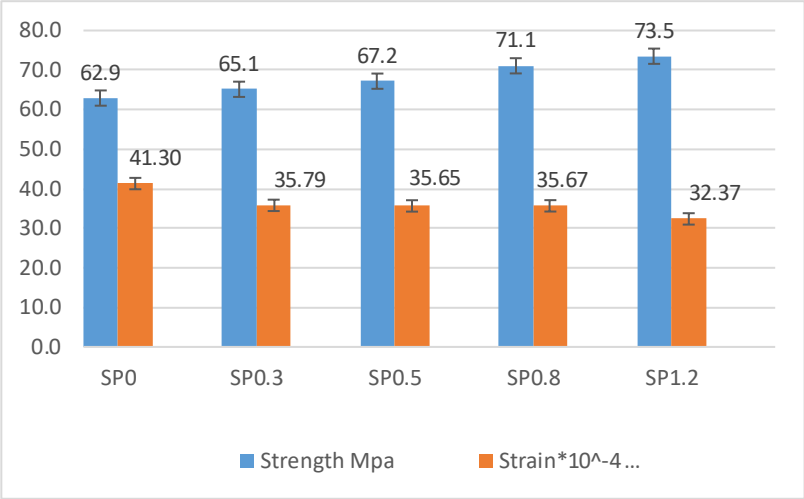

Figure 3-34, Stresses and corresponding Strains at Day 28

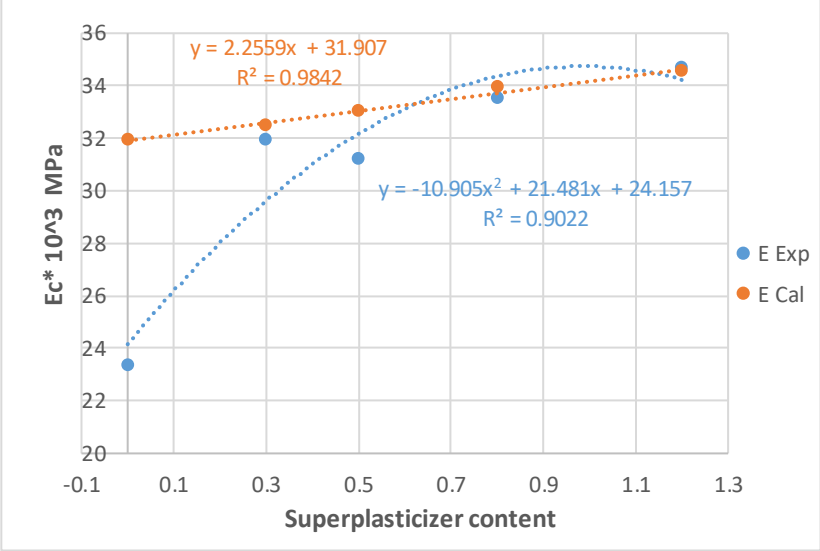

Figure 3-35, Evolution of E_c as a function of SP content

3.5.2.2.2 Cast Versus Printed Specimens

The printed specimens were tested in X, Y, and Z directions to determine the effect of printing directions on the compressive strength of the printed elements. As mentioned before, for the printed specimens, the mix that has the highest compressive strength at day 7(i.e., WC0.36 SP0.0.8) will be chosen to print the specimens with. Like the cast specimens, the same procedures

were followed for the printed ones. The compressive strength loaded in Y and Z directions were slightly different as it was expected. This can be attributed to the fact that a square nozzle was used for printing the samples, where the bonding interfaces are almost the same in both directions. While, the compressive strength in X direction was found to be the lowest with about 16% strength reduction as compared to the other directions and that could be related to the fact that the loaded area in X direction is less than the ones in Y and Z directions . On the other hand, the cast specimens exhibited higher compressive strength with difference of about 29%, 27%, and 35% when comparing it with the strength values of Y,Z, and X directions, respectively. Figure 3-36, and Figure 3-37, demonstrate the compressive strength of cast and printed specimens at the age of 7 and 28 days. These differences in compressive strength between the cast and the printed ones are related to the fact the cast specimens have higher density than the printed ones due to the voids that have been created between the printed layers by the shrinkage.

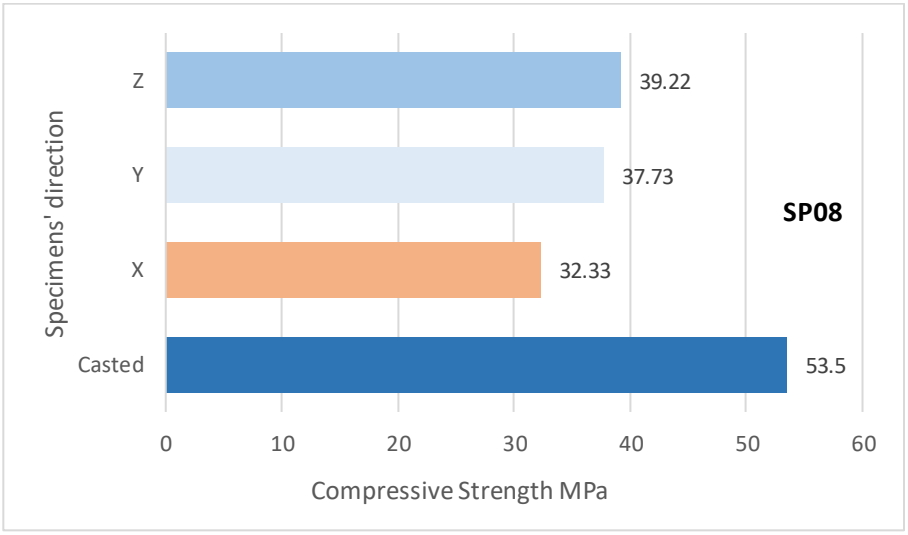

Figure 3-36, Compressive strength of printed and cast specimens at Day 7

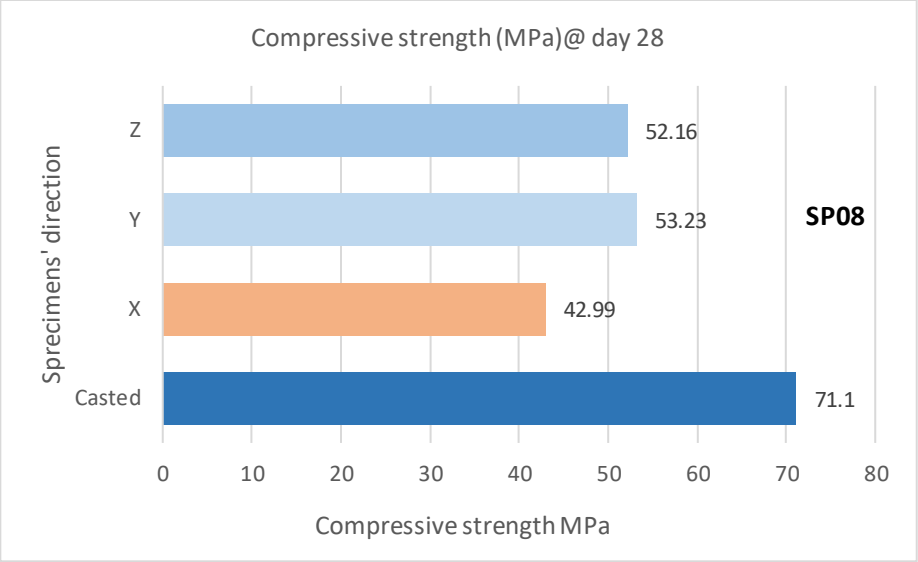

Figure 3-37, Compressive strength of printed and cast specimens at Day 28

3.5.2.3 Flexural Test

To determine the modulus of rupture for both printed and cast specimens, third point loading was used in accordance with ASTM standard (C78/C78M-18). The test method covers the determination of the flexural strength of concrete specimens using a simple beam with dimensions of 100 by 100 by 450 mm (width by height by length) and the applied loading rate was set to 3.5 KN/min. To measure the effect of different superplasticizer contents on the flexural strength of the specimens, a total of 17 specimens were tested in this research, including 15 cast specimens and two printed flexural specimens (due to the limited availability of the powder superplasticizer). Figure 3-38, demonstrates the MTS machine used for testing the flexural specimens.

Figure 3-38, MTS machine for flexural testing

The prisms were tested at the age of 28 days. Figure 3-39, illustrates a schematic of flexural testing apparatus for third-point loading method.

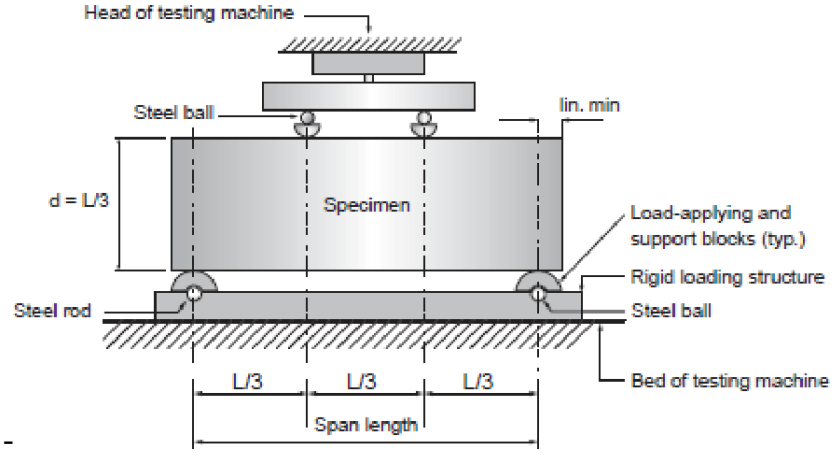

Figure 3-39, Third point- Loading method in accordance with ASTM C78/C78M- 18

Because the fracture initiates as a result of the tension induced within the middle third of the span length, the modulus of rupture can be calculated using equation 1:

$$R = \frac{P * l}{bd^2} \quad (1)$$

Where:

R= modulus of rupture, MPa
P= maximum applied load indicated by the testing machine, N
L= Span Length, mm
b= average width of specimen, mm, at the fracture
d= average depth of specimen, mm at the fracture.

3.5.2.3.1 Flexural Testing of Cast Specimens

In order to measure the effect of superplasticizer, 15 prisms specimens were cast with different quantities of superplasticizer (0, 0.3, 0.5, 0.8, and 1.2) %, three specimens were assigned for each quantity. Prisms contained SP 0.8, 1.2% of the binder content had exhibited the highest values of modulus of rupture 10.32, 10.22 MPa, respectively. While the specimens with SP 0.3, 0.5 % had expressed lower bending strength with average values of 7.83, 8.32 MPa, respectively. On the other hand, the specimens with zero superplasticizer had shown the lowest strength with an average value of 6.54 MPa. Figure 3-40, demonstrates the effect of different quantities of superplasticizer on the load- displacement curves. Figure 3-41, illustrates the average values of modulus of rupture for different ratio of superplasticizer that obtained from flexural test. It could be noticed form the former figure that the toughness property of the cast specimens increases with increasing the superplasticizer content.

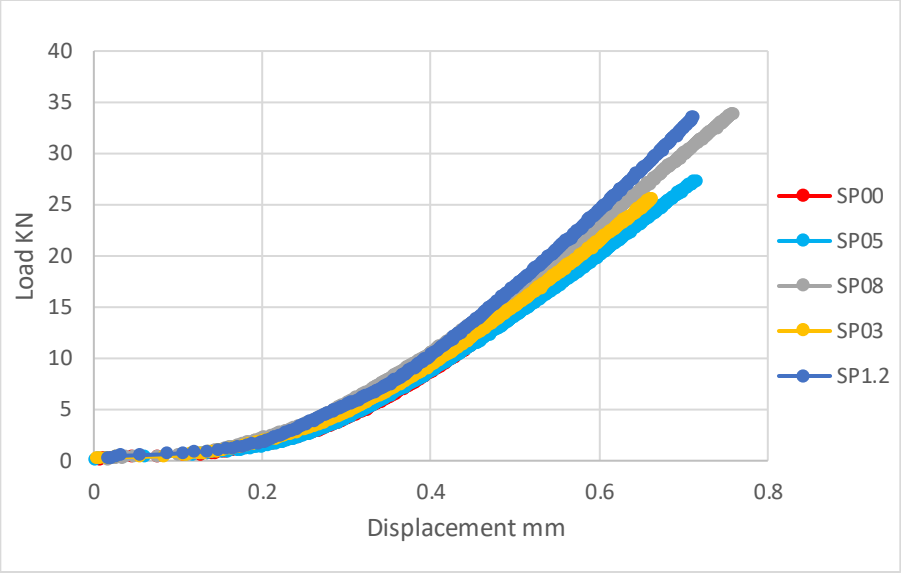

Figure 3-40, Load-displacement curves for the cast specimens

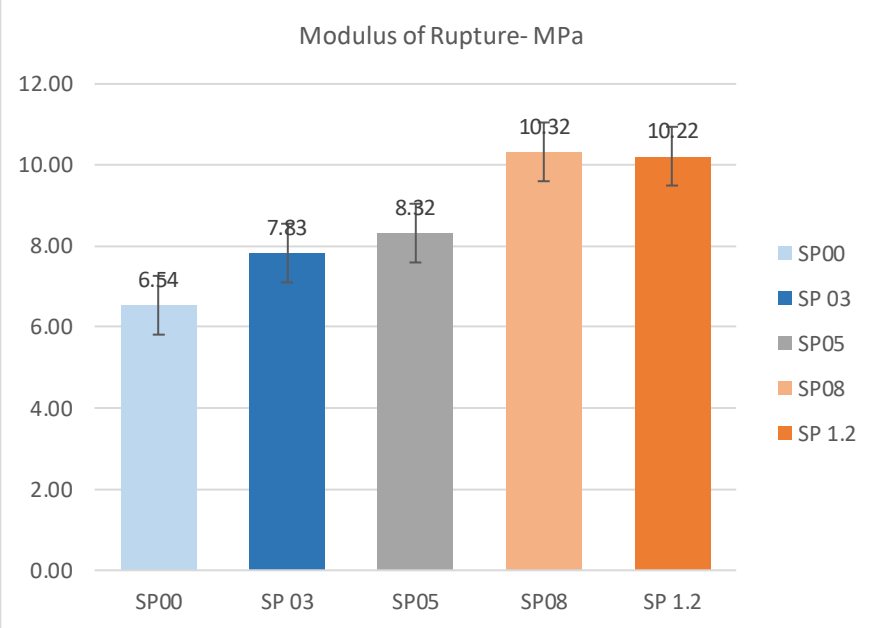

Figure 3-41, Modulus of rupture of the Cast specimens

Figure 3-42, shows the applied Loads and the corresponding displacements. The results have shown that modulus of rupture increases with increasing the superplasticizer content and that could be related to achieving higher consolidation.

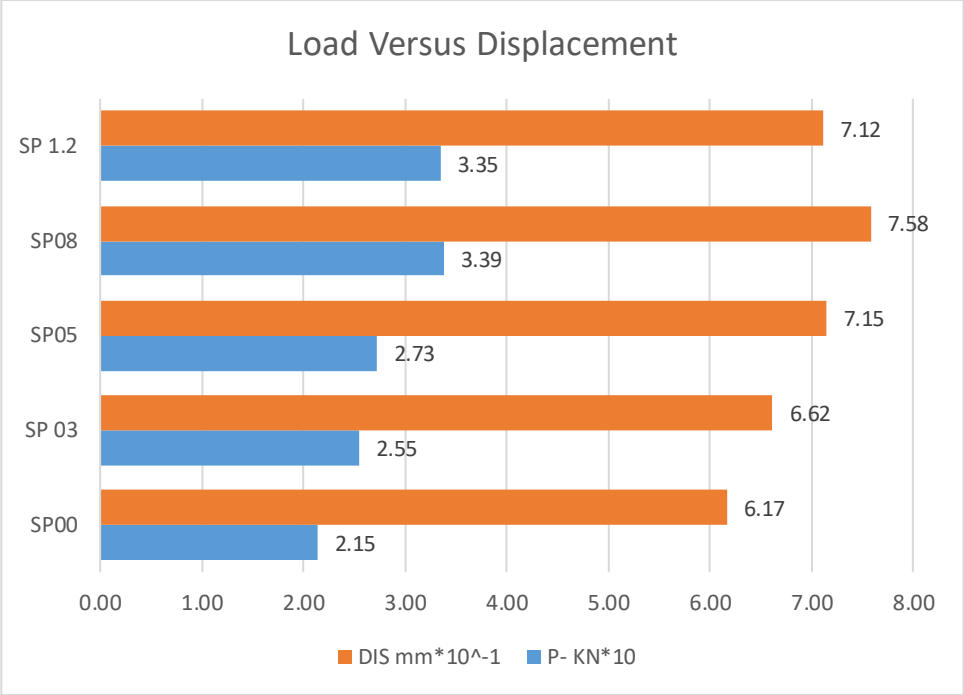

Figure 3-42, Load and corresponding displacement

However, the effect of superplasticizer content on the modulus of rupture seems to be the same after reaching 0.8% of the binder content, which means the optimum consolidation is achieved with the former percentage of superplasticizer.

3.5.2.3.2 3D Printed Flexural Specimens

A rectangular nozzle (30 * 15 mm) was used for printed flexural specimens, allowing the size effects of the nozzle and the bond strength among the layers to be observed on the bending strength. Like the compressive specimens, the printed prisms were done using SP 0.8 %. Fig 3-43, shows the printed specimens using the rectangular nozzle.

Figure 3-43, Printed flexural specimens

The printed specimens were tested in (Y, Z) directions to determine the effect of printing directions on the flexural strength. The Load along with Z direction was significantly higher than the one applied on Y direction with more than 39% as it can be seen from Figure 3-44. The higher strength achieved with Z direction is related to the fact that the bond strength along with Z direction (blue highlighted lines) consider to be weakness points which lead the printed filaments to act as one filament in Z direction (b= 30 mm, h= 100 mm, Iz= 8.3*10^6 mm4). On the other hand, when the load is applied on Y direction, the stiffness of the printed filament is (b= 100 mm, h= 30 mm, Iy= 6.83*10^5 mm4) which resulted in lower stiffness to resist the bending strength. Figure 3-45, illustrates the adhesion areas among the layers (blue highlighted lines= weak joints, red highlighted lines= strong joints).

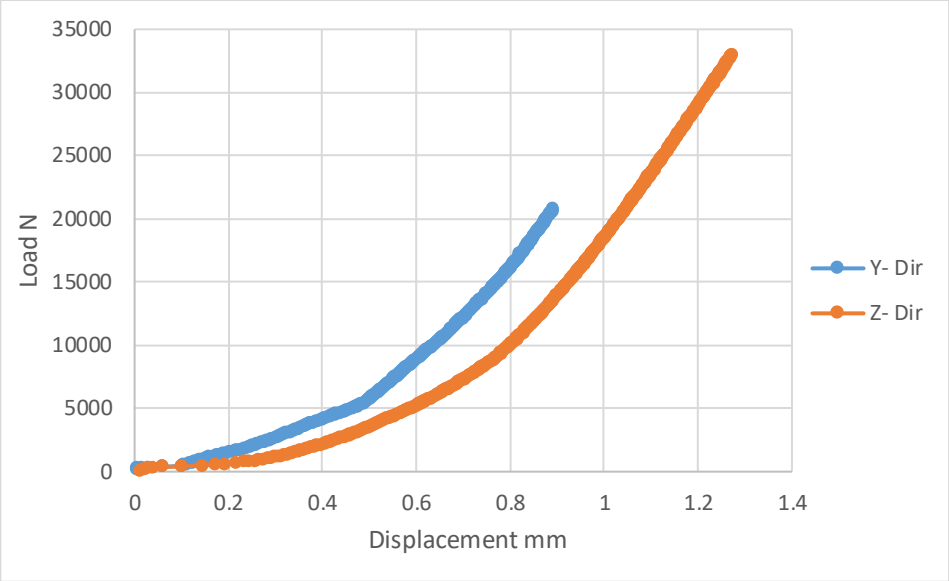

Figure 3-44, Load and Displacement curve

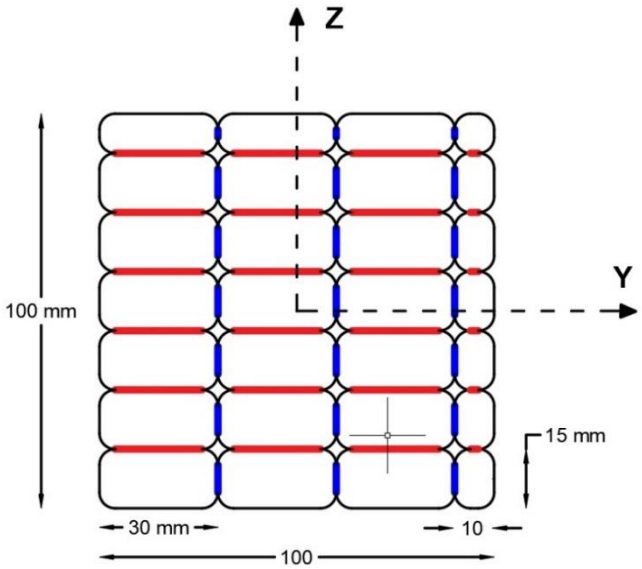

Figure 3-45, Adhesion areas between the printed filaments

To this end, the modulus of rupture on Z direction is higher than the one on Y direction with more than 42 %. Although the flexural stiffness that is represented it by the slope of the load deflection curve has expressed the same stiffness for both direction Y,Z , the absorbed energy to the fracture state “Toughness” that affined with specimen that loaded on Z direction is significantly

higher than the one affined with Y direction with more than 55%. Figure 3-46, demonstrates the modulus of rupture of the printed specimens in both directions (Y, Z).

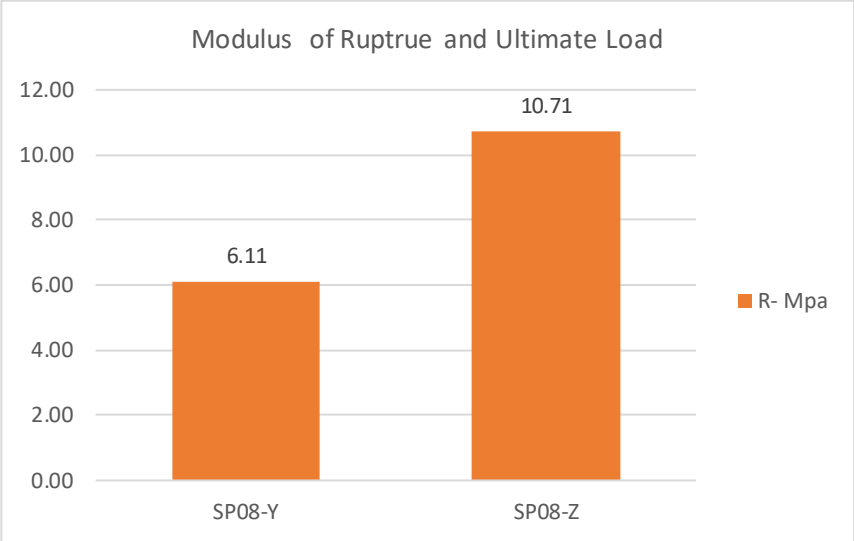

Figure 3-46, Modulus of rupture of the printed Specimens in (Y, Z) directions

3.5.2.3.2.1 Cast Specimens Versus the Printed Ones

The modulus of rupture of the printed specimen on Z direction has shown almost the same strength when it is compared with the cast specimens that contain SP 0.8%. While the modulus of rupture on Y direction expresses reduction in strength comparing with the cast specimens by 40%. Figure 3-47, exhibits the Load and displacement curves for the printed and cast specimens. It could be noticed form this figure that amount of absorbed energy to the fracture load that affined with Z direction is higher than the ones that linked with Y direction and the cast specimens by 55% and 42%, respectively. However, the cast specimens and the printed ones express the same flexural stiffness. Figure 3-48, demonstrates the modulus of rupture with the corresponding loads and displacements for both printed and cast specimens. To this end, the results of flexural test on the printed prisms have shown a sever anisotropic behavior depending on the load direction and that could be related to the fact that the printed layers on Z direction have stronger bond strength than those printed on Y direction due to two main factors, 1). Bigger interfaces area achieved between the layers, 2). Better compaction achieved due to the weight of the subsequent layers.

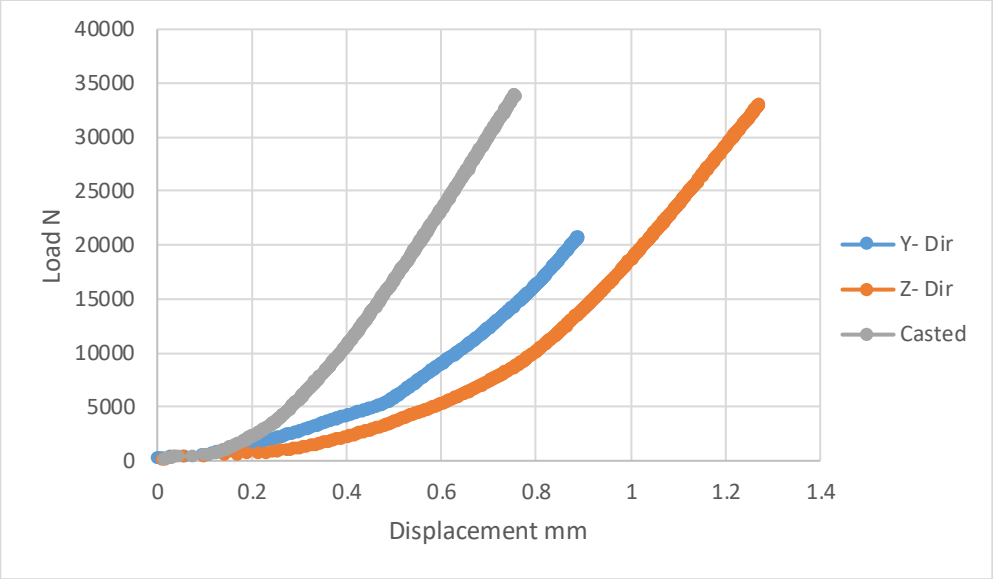

Figure 3-47, Load and displacement curve for cast and printed specimens

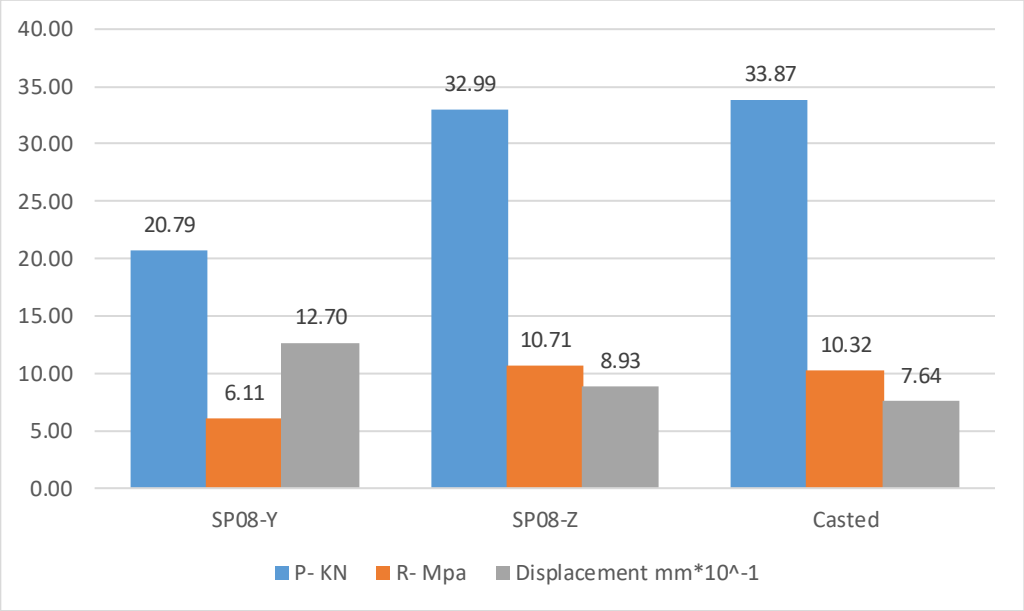

Figure 3-48, Load, modulus of rupture, and Displacements for Cast and Printed specimens

Moreover, by obtaining the flexural strength of the cast and printed samples, the tensile could be derived from the modulus of rupture. Different experimental studies show that there is a reduction in the tensile strength by (20 to 40) % of the flexural strength, depending on the

water cement ratio, aggregates grades, and SCM percentage (Olanike, 2014) (Salem, 1996) (Troxell, Davis, & Kelly, 1968) (Ravindrarajah & Tam, 1985).

Chapter 4: Conclusion

4.1 Conclusion and Recommendations

A 3D printable concrete mixes, mainly using domestically available raw materials, was developed in this research. To investigate the feasibility of using GGBFS in developing 3D-Printable mixes, 12 concrete mixes were evaluated with respect to printability, buildability, fresh and hardened properties. The effect of superplasticizer content on the rheological behavior of fresh and hardened concrete specimens was further evaluated to fine-tune the 3DCP mix design. This investigation yielded a number of intriguing discoveries, which are mentioned below:

- The observed pattern of variations in shear strength as a function of superplasticizer content was found to be consistent with the literature, which shows that strength and admixture ratio have an indirect exponentially proportional relationship.
- Using the established platform at UW, the best shear strength range for creating acceptable 3D-Printable concrete mixtures is [0.23-0.44] kPa. Wet mixtures (extrudable but not buildable) are considered below 0.23 kPa, whereas stiff mixes are considered above 0.44 KPa (Unprintable).
- WC0.36SP0.50 and WC0.36SP0.80 have the highest printability quality. The proposed wall was printed by using WC0.36SP0.50, while the specimens were printed using WC0.36SP0.80.
- The height and section of the nozzle have a major impact on the printing quality. Square and rectangular cross sections lead to better buildability than circular cross sections. Also, it was observed that the ideal height for extruding the filaments is (Nozzle height + 2 to 5 mm), otherwise the printed would not line vertically well.
- The cast specimens containing SP 0.8 % of the binder content attained their greatest compressive and flexural strengths, whereas those containing SP 1.2 % showed no strength improvements. The most absorbed energy to the fracture point, on the other hand, has

affined with the former. However, specimens with an SP 1.2% are considered extremely moist to print with.

- The compressive strengths of the printed specimens showed anisotropic behavior dependent on the load directions. It was discovered that specimens loaded in the X direction have the lowest compressive strength when compared to those loaded in the Y and Z orientations, with a strength reduction of 16%.
- Regardless the printing directions, the printed specimens have exhibited lower compressive strength than the cast ones with a strength reduction ranging from 26 % to 35%, depending on the load directions.
- Nozzle's cross section and the printing direction have a significant influence on the flexural strength. The modulus of rupture on Z direction is higher than the one on Y direction with more than 42 %.
- Although the cast specimens with SP0.8% and the printed ones on Z directions have expressed almost the same modulus of rupture and flexural stiffness, the printed on ones on Z direction exhibited higher toughness than the cast ones with an energy increase up to 42%.

To this end, the findings of this research have aligned with the ones that reported in literatures reviews such as, (Panda, Chandra Paul, Jian Hui, Daniel Tay, & Jen Tan, 2017) , (Rahul, Santhanam, Meena, & Ghani, 2019), , (Le, et al., 2012). 3D- concrete printing consider to be a new technology approach in constructions fields. And many parameters could have significant influences on the printing quality, such as robotic parameters, mixes' ingredients and admixtures, so further investigations are needed to determine the effect of these parameters and come up with comprehensive codes and standards that set a worldwide foundations of 3D- Concrete printing.

4.2 Recommendation and future research directions

In the laboratory test procedure that was used to investigate the buildability of the fresh concrete, a visual evaluation was adopted which leads to consume a huge quaintly of materials and increase the expense of the research. Therefore, it would be more sufficient and useful to adopt a new method that contribute in saving more research's materials and cost such as, squeeze flow

test, which could lead us to a deeper understanding on the correlation between the applied load and the buildability property using small materials' quantities. Due to silica reaction and the high friction between the stator and its chamber, the delivery system was overheated which leaded to shut down the system a couple of times during the printing process and decrease the setting time of the concrete. Therefore, it is recommended to supply the wet chamber with a cooling system to reduce the amount of produced heat.

For future research directions, there are some suggestions that need further investigation, as listed below:

i. Optimize the use of fibers along with superplasticizer and investigate the influence on the printing quality and hardened concrete property.
ii. Scrutinize printing walls with different cross patterns on the flexural strength property.
iii. Investigate the effect of different sets of printing speed on the bond strength using SP0.5% and SP 0.8% of the binder content.
iv. Investigate new methods to reinforce the printed layers to improve the mechanical properties of the printable mixes.

References

Olanike, A. O. (2014). A Comparative Analysis of Modulus of Rupture and Splitting Tensile Strength of Recycled Aggregate Concrete. American Journal of Engineering Research, 141-147.

Al Jassmi, H., Al Najjar, F., & Mourad, A.-H. I. (2018). Large-Scale 3D Printing: The Way Forward. IOP Conf. Series: Materials Science and Engineering 324.

Buswell, R., C. Soar, R., AGibb, l. G., & Thorpeb, A. (2007). Freeform Construction: Mega-scale Rapid Manufacturing for construction. Automation in Construction, pp. 224-231.

Cardoso, F., Grandes, F., Sakano, V., Rego, A., & Pileggi, R. (2018). Squeeze flow of cement-based mortars: assessment of pressure distribution by dynamic mapping. Rheology of Building Materials.

Carolo, L. (2020, July 19). 3D Printed House: 20 Most Important Projects. Retrieved from ALL3DP.

Dini, E. (2006). D- Shape. London: www.d-shape.com.

ELLIOTT, A., & WATERS, C. (2019). Additive manufacturing for designers : A primer.

Ghaffar, S., Fan, M., & Corker, J. (2018, September). Additive manufacturing technology and its implementation in construction as an eco-innovative solution. Automation in Construction.

Guowei, M., Junfei, Z., Li, W., Zhijian, L., & Junbo, S. (2018). Mechanical characterization of 3D printed anisotropic cementitious material by the electromechanical transducer. Smart Materials and Structures.

Hogan, F., & Meusel, J. (1981). Evaluation for durabilityand strength development of a ground granulated blast furnaceslag,. Cement, Concrete and Aggregates, 40-52.

Hwang, D., & Khoshnevis, B. (2005, September 11). An Innovative Construction Process-Contour Crafting(CC). Automation and Robotics in Construction.

Jeong, H., Han , S.-J., Choi , S.-H., Lee, Y., Yi, S., & Kim , K. (2019, January 7). Rheological Property Criteria for Buildable 3D Printing Concrete. Concrete 3D Printing and Digitally-Aided Fabrication.

Jianchao, Z., Zhang, T., Faried, M., & Wengang, C. (2017). 3D printing cement based ink, and it's application within the consruction industry. MATEC Web of Conferences.

Kaszyńska, M., Hoffmann, M., Skibicki, S., & Zieliński, A. (2018). Evaluation of suitability for 3D printing of high performance concretes. MATEC web of conferences.

Khoshnevis, B. (2004). Automated construction by contour crafting—related robotics. Automation in Construction , pp. 5-19.

KOVÁŘÍK, M., SVOBODA, P., & ACHTEN, H. (2019, February 4). Limits and Potential of 3D Printing Technologies for Construction of concrete shells. Trans Tech Publications Ltd, Switzerland.

Krishna , V. B., Roberson , L. B., O'Connor, G. W., Trigwell, S., & Bose, S. (2012). First demonstration on direct laser fabrication of lunar regolith parts. Rapid Prototyping , 451-457.

Labonnote, N., Rønnquist, A., Manum, B., & Rüther, P. (2016). Additive construction: State-of-the-art, challenges and opportunities. Automation in Construction, pp. 347-366.

Lafarge. (n.d.). NewCem. Retrieved from Lafarge.ca: https://www.lafarge.ca/en/newcem

Le, T. T., Austin, S., Lim, S., Buswell, R., Gibb, A., & Thorpe, T. (2012). Mix design and fresh properties for high-performance. Materials and Structures.

Lim, S., Hussin, M., & Ling, T.-C. (2012, March). Strength properties of self-compacting mortar mixed with GGBFS. Construction Materials, pp. 165(2):87-98.

Lim, S., Le, T., Webster, J., Buswell, R., Austin, S., Gibb, A., & Thorpe, T. (2009). FABRICATING CONSTRUCTION COMPONENTS USING LAYERED MANUFACTURING TECHNOLOGY.

Nerella, V., Näther, M., Iqbal, A., Butler, M., & Mechtcherine, V. (2018, December). Inline quantification of extrudability of cementitious materials for digital construction. Cement and Comncrete composition.

Neville, A. (2010). Concrete Technology. Tottenham: British Library .

Ozalp, F., & Yilmaz, H. D. (2020). Freash and Hardened Properties of 3D High- Strength Printing Concrete and its Recent Applications. ResearchGate.

Pan, T., Jiang, Y., He, H., Wang, Y., & Yin, K. (2020). Effect of Structural Build-Up on Interlayer Bond Strength of 3DPrinted Cement Mortars. MDPI.

Panda, B., Chandra Paul, S., Jian Hui, L., Daniel Tay, Y. W., & Jen Tan, M. (2017). Additive manufacturing of geopolymer for sustainable built. Elsevier, 281-288.

Paul, S. C., Tay, Y. D., Panda, B., & Tan, M. J. (2018). Fresh and hardened properties of 3D printable cementitious materials for building and construction. Archives of Civil and Mechanical Engineering.

Penga, J. (1997). Exploratory investigation of solid freeform construction. Automation in Construction, pp. 427-437.

Ph, R., R, D., C, G., N, G., J, D., & Ph, M. (2016). Large-scale 3D printing of ultra-high performanceconcrete – a new processing route for architects and builders. HAL.

Rael, R., & San Fratello, V. (2011). Developing Concrete Polymer building components for 3D printing. ACADIA (pp. 152-157). Calgay/Banff, Canada: Annual conference Aided Design in Archetictural .

Rahul, A., Santhanam, M., Meena, H., & Ghani, Z. (2019). Mechanical characterization of 3D printable concrete.

Ravindrarajah, R., & Tam, C. (1985). Properties of concrete made with crushed concrete as coarse aggregate. ICE.

Salem, M. R. (1996). Strength and Durability Characteristics of Recycled Aggregate. Knoxville : University of Tennessee.

Shakor, P., Renneberg, J., Nejadi, S., & Paul, G. (2017). Optimisation of Different Concrete Mix Designs for 3D Printing by Utilizing 6DOF Industrial Robot. The International Association for Automation and Robotics in Construction.

Shelley, T. (2006). Maximum material performance . Eureka.

Singh, S. (2014, September 8). Minimization of form errors in additive manufacturing. Retrieved from Slideshare: https://www.slideshare.net/sanjeev13apr/minimization-of-form-errors-in-additive-manufacturing?from_action=save

T, T., A.G.F. , G., S.A, A., T.T. , L., R.A. , B., & S, L. (2012). Developments in construction-scale additive manufacturing processes. Automation in Construction, pp. 262-268.

Thomas, M. (2007). Optimizing the Use of Fly Ash in Concrete. New Brunswick: University of New Brunswick.

Tofail, S. A., Koumoulos, E. P., Bandyopadhyay, A., Bose, S., O'Donoghue, L., & Charitidis, C. (2017). Additive manufacturing: scientific andtechnological challenges, market uptake and opportunities. ScienceDirect.

Troxell, G. E., Davis, H. E., & Kelly, J. W. (1968). Composition and properties of concrete. Newwrok: McGraw-Hill.

Wilhelm, S., & Curbach, M. (2014). Review of possible mineral materialsand production techniques for a buildingmaterial on the moon. Structural Concrete, 419-428.

Wolfs, R., Bos, F., & Salet, T. (2018, April). Early age mechanical behaviour of 3D printed concrete: Numerical modelling and experimental testing. Cement and Concrete Research, pp. 103-116.

Wolfs, R., Bos, F., & Salet, T. (2019). Hardened properties of 3D printed concrete: the influence of process parameters on interlayer adhesion. Cement and Concrete Research, 132-140.

Zhang, J., Wang, J., Donga, S., Yu, X., & Han, B. (2019, Septmeber). A review of the current progress and application of 3D printed concrete. ELSEVIER.

Zhu, B., Pan, J., Nematollah, B., Zhou, Z., Zhang, Y., & Sanjayan, J. (2019). Development of 3D printable engineered cementitious composites withultra-high tensile ductility for digital construction. ElSEVIER.

Appendix A

Testing Type: Date : 11/13/2019

Specific Gravity & Absorption[C 128-15]

Two samples had been conducted in accordance with **ASTM C128-15** to determine the Specific Gravity and Absorption content of fine Sand, by following the Gravimetric procedures.

Apparatus:

- Flask 500 ml
- Mold and Tamper
- Oven 110 ±5°C
- Balance
- Gun Heating

Equations:

Absorption% = $(S - A)/A * 100$

Specific Gravity = $S1/(R1 + S1 - R2)$

Whereas:

A= mass of oven dry

S= mass of saturated surface dry specimen

S_1= mass of saturated surface dry specimen used in Flask

R_1= mass of water level in Flask

R_2= mass of water level in Flask with sand.

Sample 1	**Sample 2**
S_1= 55.5 g	S_1= 55.6 g
S= 445.2 g	S= 404.4 g
R_1= 496.1 g	R_1= 496 g
R_2= 531.2 g	R_2= 531.9 g
A= 441.8 g	A= 402.1 g
Absorption= 0.7%	Absorption= 0.57%
S.G= 2.72	S.G= 2.82

Average:

Absorption = 0.635 %

S.G= 2.77